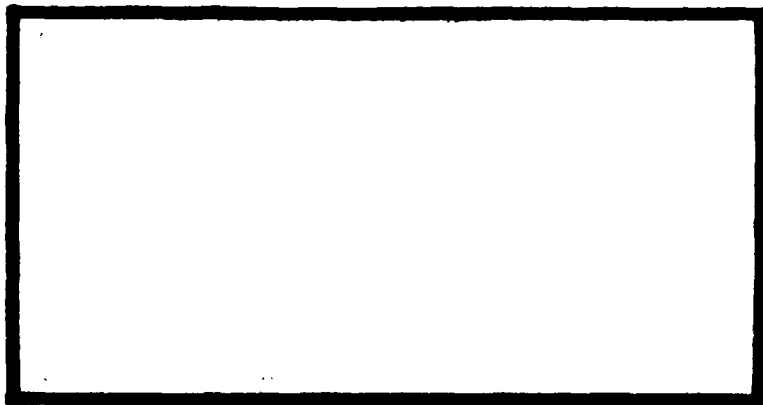


AD A094813



LEVEL II

①



DTIC
ELECTE
S FEB 10 1981

DEPARTMENT OF THE AIR FORCE
AIR UNIVERSITY (ATC)
AIR FORCE INSTITUTE OF TECHNOLOGY

Wright-Patterson Air Force Base, Ohio

DISTRIBUTION STATEMENT A

Approved for public release;
Distribution Unlimited

81 2 09 051

DOC FILE-CURVED

AFIT/GEO/PH/80D-9

APPROVED FOR PUBLIC RELEASE AFR 190-17.

27 JAN 1981

Laurel A. Lampela
LAUREL A. LAMPELA, 2d Lt, USAF
Deputy Director, Public Affairs

①

Assistant Professor of Technology (ATC)
Wright Patterson AFB, OH 45433

LEVEL II

① TRADE-OFF ANALYSIS OF WAVELENGTHS
FOR TACTICAL ELECTRO-OPTICAL AIR-TO-GROUND
WEAPON SYSTEMS.

THESIS

AFIT/GEO/PH/80D-9

① Gregory A. Mullins
Civilian USAF

TRADE-OFF ANALYSIS OF WAVELENGTHS
FOR TACTICAL ELECTRO-OPTICAL AIR-TO-GROUND
WEAPON SYSTEMS

THESIS

Presented to the Faculty of the School of Engineering
of the Air Force Institute of Technology
Air University

in Partial Fulfillment of the
Requirements for the Degree of
Master of Science

Accession For	
DTIC	X
EDIC	
Unannounced	
Justification	

A

by
Gregory A. Mullins, B.S.
Civilian USAF
Graduate Electro-Optics
December 1980

Approved for public release; distribution unlimited.

Preface

This trade-off analysis was performed with the intent of identifying the electro-optical wavelength providing the greatest inherent benefit to the Air Force for air-to-ground weapon delivery applications. Such an analysis depends heavily on the selection of the operational requirements and constraints used. I recommend, therefore, that the reader of this thesis carefully reviews and understands the assumptions and limitations given in this thesis.

I would like to extend my appreciation to my advisor, Dr. D. Shankland, for his patience and guidance in such a multi-faceted problem. Also, I want to thank Dr. B. Kulp for his views and insights into the basic tactical requirements of the Air Force.

The help I received from Ray Wasky, Bill Harmon, Tom Porubcansky, Ray Rang, Capt. Bill Smith and Capt. Ray Lacotta of the Avionics Lab is greatly appreciated. Others who provided valuable information were Maj. Bob Davies of the A-10 SPO, Maj. Ray Huit of TAC/DRA, Rich Davis from ASD/ENAMB, Tony Elam from the Pave Tack SPO and Roger Brislawn of the LANTIRN SPO.

My special thanks, however, go to my wife, Pam, for her infinite understanding and patience during the development of this thesis.

Contents

	Page
Preface	ii
List of Figures	v
List of Tables	vii
Abstract	viii
I. Introduction	1
Objective	1
Scope	2
Assumptions	3
Background	4
Organization	7
II. Air Force Requirements	9
Scenario	9
Defining Critical Parameters	18
Smoke	22
Weather	24
CEP	24
Pod Diameter	29
System Utility Function	30
III. Nd:YAG Designation System	38
Weather Penetration	38
Smoke Penetration	46
Spot Size	47
Pod Diameter	48
IV. CO ₂ Designation System	49
Weather Penetration	49
Smoke Penetration	51
Spot Size	51
Pod Diameter	51
V. Millimeter Wave Designation System	53
Weather Penetration	53
Smoke Penetration	57
Spot Size	57
Pod Diameter	58

Contents

	Page
VI. Results	59
VII. Conclusion	62
Observations	62
Recommendations	64
Bibliography	65

List of Figures

<u>Figure</u>		<u>Page</u>
1	Typical Soviet Deployment Concept	11
2	Soviet T-72 Tank	12
3	Soviet ZSU-23/4 Mobile Antiaircraft Vehicle	12
4	Attack Suppression Scenario	13
5	Mean Number of Hours per Year Precipitation Rate is Exceeded	15
6	Frequency of Fog	15
7	Maximum Duration of Fog (Visibility \leq 1km)	16
8	Smoke Scenario	17
9	Visual Attenuation Through Various Smokes	18
10	Utility Function for Smoke Scenario	22
11	Utility Function for Probability of Hit	25
12	Relationship Between CEP and Probability of Hit	26
13	Utility Function for CEP	27
14	Utility Function for Spot Size	29
15	Pod Size and Weight Impacts on F-16 Aircraft Performance Side Inlet and Centerline Location	31
16	F-16 External Store Capability	32
17	Utility Function for Pod Diameter	33
18	Probability of Detection vs SNR for $n = 2 \times 10^9$ and $N = 1$	42

List of Figures

<u>Figure</u>		<u>Page</u>
19	Typical Detectivities for Various Near Infrared Detectors	43
20	Fog/Haze Scenario	44
21	Wind Speed vs Probability of Occurrence	45
22	Dew Point vs Probability of Occurrence	45
23	Detectivities for Infrared Sensors	49
24	Example of Negative Utility	61

List of Tables

<u>Table</u>		<u>Page</u>
I	Potential Soviet Targets	10
II	Soviet Target Distribution	11
III	Distribution of Key Air Defenses	11
IV	Atmospheric Attenuation Coefficients for 1.06 μm . . .	44
V	Atmospheric Attenuation Coefficients for 10.6 μm . . .	50
VI	Atmospheric Attenuation Coefficients for 94 GHz . . .	55
VII	Utility Values for Candidate Systems	59

Abstract

A trade-off analysis was conducted for various electro-optical wavelengths as candidates for the next-generation air-to-ground electro-optical weapon system. The three candidates considered were 1.06 μm (Nd:YAG), 10.6 μm (CO_2) and millimeter wave (94 GHz). Specific Air Force requirements were defined in order to perform this analysis. These requirements included the expected battlefield scenario and the most critical weapon system performance parameters.

The battlefield scenario used was an interdiction operation against a high concentration of small hardened targets in Central Europe. The attacking aircraft was assumed to be of the A-10, F-16 variety carrying an armor-piercing missile such as the Maverick with a shaped charge warhead. It was assumed that the missile employs a point-tracking, semi-active seeker which homes-in on target-reflected energy originating from a designator collocated with the missile on the aircraft.

Decision theory was used to quantize the trade-off analysis by selecting the most critical performance parameters and establishing, not only relative weighting between the parameters, but also utility functions for each of the parameters. The parameters selected were detection range in adverse weather, detection range in tactically deployed smoke, designator spot size on the intended target and the designator pod diameter. Transmission data for haze, fog and white phosphorus smoke established the detection ranges for the candidate

wavelengths while calculated beam divergence defined the spot size and values from existing and proposed designation systems defined the pod diameter.

By only addressing the radiation return from the intended target, i.e., assuming the appropriate spatial and temporal filtering is provided in the receiver, the analysis resulted in showing the CO₂ system as having the highest potential benefit to the Air Force for the specified application. It was followed by the Nd:YAG system and then the millimeter wave system.

It was observed that by considering a different type of ordnance such as a guided bomb, the dependence on spot size would be less severe and the millimeter wave system's longer detection ranges could potentially increase its utility over that of the other systems. It was recommended that the scope of this analysis be expanded to include other weapon delivery concepts such as beam rider missiles and that background radiation effects be included.

I Introduction

Objective

The current status of the United States Air Force tactical weapon delivery capability disproves the old military adage of "What can be seen, can be destroyed." Recent incorporation of imaging infrared sensors into the Air Force inventory has extended the detection ranges of air-to-ground weapon systems against tactical targets in several battlefield scenarios. The launch ranges of many of the guided weapon systems still being used, however, are limited to inherent atmospheric penetration characteristics of the guidance wavelengths. The discrepancy between detection range and weapon delivery range is of concern to the Air Force and is being addressed by an effort to improve the range performance of air-to-ground weapon systems. Various electro-optical wavelengths are being investigated for possible applications and improvements to tactical weapon delivery (Ref 11).

The objective of this thesis, therefore, is to perform a trade-off analysis on selected wavelengths based upon their desirability and suitability as guidance wavelengths for air-to-ground weapon delivery. This analysis is structured to quantify the relative utility of the candidate wavelengths by developing and using an Air Force requirements decision model. This approach simplifies the trade-off problem to one of comparing a single figure of merit for each system and identifies the technical area with the greatest potential benefit.

Scope

This thesis deals only with the Air Force requirements for electro-optical systems as they apply to air-to-ground weapon delivery. These requirements originate from the Air Force mission of close air support and interdiction. In this context, therefore, the airborne platform used for this study is a low altitude aircraft such as the A-10 or F-16. This platform is considered to be operating in a high threat environment in central Europe where several small, hardened targets (tanks, armored personnel carriers (APC), etc.) exist for each aircraft. A high probability of hit is required for any weapon system being used. For this reason, only active systems utilizing a semi-active seeker on the weapon are considered in this thesis because of two inherent accuracy advantages. These advantages are the control of the target signature and the fact that active systems are convergent systems, i.e., the guidance error of the weapon decreases as it approaches the target. This is in contrast to divergent weapon delivery approaches, such as beam rider systems where guidance error depends on the angular tracking error of the airborne designator and, therefore, increases as the aircraft-to-weapon range increases.

The type of weapon addressed in this thesis is an air-to-ground, powered missile which contains some sort of armor penetration capability (such as the Maverick missile). Representative parameters for this type of missile are used in this thesis for the required calculations.

The choice of the wavelengths considered in this study is based on the current state-of-the-art of various electro-optical devices and on the amount of supporting data, both theoretical and experimental, available. The two devices receiving the most attention within the Air Force are CO₂ lasers (10.6 μm wavelength) and millimeter wave devices (25 to 220 GHz frequency). These candidates for the next generation electro-optical device have demonstrated definite potential for improving weapon delivery capability over that now offered by Nd:YAG (1.06 μm) systems. For this reason, and since more data exists at these wavelengths than at other wavelengths, this thesis examines the CO₂ devices and a representative millimeter wave device (94 GHz). Also, similar calculations are performed for the Nd:YAG systems in order to form a baseline for comparison.

Assumptions

Since this study deals with systems which will require much development before being introduced into the Air Force inventory, it is assumed that the associated electronics can be designed to adequately process the available guidance signal. Only the optical and electro-optical properties of the various wavelengths, therefore, are considered in this study. This assumption is valid since the processing schemes designed for existing 1.06 μm systems do not depend on the system's wavelength, but rather on the form of the converted electrical signal from the receiver. Such schemes include wide-pulse logic which discriminates against backscatter reflections from the atmosphere.

Additional assumptions are addressed in their relevant sections for clarity and for ease of substantiation.

Background

As stated previously, one of the primary roles of the United States Air Force in a conventional, tactical war is that of close air support and interdiction. This mission requires the efficient elimination of an enemy threat while maintaining the maximum possible survivability of the attacking aircraft. The Air Force must be equipped, therefore, with the means to identify enemy targets and to direct sufficient firepower on these targets from "safe" ranges and altitudes. Electro-optical devices have been used by the Air Force in trying to fulfill this requirement. These devices can be divided into two types; passive devices and active devices.

Passive devices depend solely on emitted radiation generated by the target or on reflected radiation originating from natural sources. Two types of passive devices used by the Air Force are television sensors and Forward-Looking InfraRed Sensors (FLIRs).

Television sensors respond only to the visible wavelength spectrum of 390 nanometers to 770 nanometers (Ref 24:3-3). The emitted or reflected target radiation is detected by the television sensor and converted to an electrical representation of the target scene. Since this type of sensor does not enlarge the detectable wavelength range over that of the eye, the only enhancement realized is one of image magnification.

Due to the large technology cross-over from the commercial television industry, and the maturity of the technology, television sensors have been used extensively by the Air Force for both target

detection and weapon delivery. Two examples of television systems in the inventory are the Pave Spike acquisition and target designation pod (AVQ-23) which uses a television sensor for target search and detection and the television Maverick air-to-ground missile (AGM-65B) which homes-in on a target by tracking its television image. Although these systems provide a significant improvement over visual detection of targets and ballistic weapon delivery, range dependence on atmospheric attenuation and on target visual characteristics severely limits their tactical utility.

FLIR systems are simply television sensors which operate in the far infrared spectrum. While some systems have been developed in the 3-5 μm range, all systems now in the Air Force inventory or undergoing engineering development operate in the 8-12 μm range (Ref 11). *The detected energy level of radiation in these spectra is directly related to the thermal emittance of the target. This allows the FLIR to identify and track targets, based not on their visual contrast with the background, but on their thermal differential with the background. This characteristic not only increases the types of targets detectable, but also makes use of greater atmosphere transmission over that encountered in the visual spectrum. FLIRs allow, therefore, larger stand-off ranges than those for television sensors. The detector technology for infrared systems, however, is not nearly as advanced as those operating in the visual spectrum (Ref 19:4). This requires, therefore, more sophisticated methods of detecting the infrared radiation and converting it to a usable electrical signal. The approach commonly used is to reflect the target image on to the infrared detector*

by using a revolving carousel of mirrors. The pitch of these mirrors is controlled so as to reproduce the target scene in the form of the standard television raster scan. Such technology has been used in the development of the Pave Tack FLIR (AN/AAQ-9) and the Imaging Infrared Maverick Missile (AGM-65D). These systems still suffer from the inherent disadvantage of passive devices, however, in that the target signature is not controllable by the weapon system.

Active weapon systems represent a method whereby the target signature can be controlled. This is accomplished by using a non-dispensable marking device, such as an aircraft mounted airborne laser, in conjunction with a semi-active (receiver only) seeker integrated with the deliverable weapon. The Air Force has used active systems since 1968 when a Nd:Glass laser designator (Pave Knife) was used with the Laser Guided Bomb (LGB) in Southeast Asia (Ref 7). This weapon system demonstrated the accuracy achievable by using the active weapon delivery scheme. Since that time, several systems have been deployed with the Nd:Glass and Nd:YAG lasers in concert with the appropriate 1.06 μm sensors. These devices retain the basic concept of illuminating the intended target with laser radiation and then tracking the reflected energy with the semi-active laser seeker. Advances made in the active weapon systems are mainly associated with refining their operation in terms of designator electrical efficiency, beam characteristics, and seeker sensitivity. Two examples of the current state-of-the-art in 1.06 μm tactical weapon systems are the Pave Tack designator pod used on the F-4 aircraft and the Laser Guided

Bomb. The Pave Tack system uses its FLIR for target identification and its Nd:YAG laser for target marking.

As stated earlier, however, a severe limitation of this approach is that, for most scenarios, the FLIR provides greater stand-off range capability than the Nd:YAG laser. This condition, therefore, establishes an inconsistency between where a target can be detected and where a weapon can be deployed.

The inconsistency between detectable targets and destroyable targets has been recognized by the Air Force community and is now being investigated. Discussions on the requirements for the next generation FLIR and laser systems have been conducted over the past three years during the USAF Armament and Avionics Planning Conference (Ref 11;21:4-195; and 22:4-205). These yearly meetings have generated several questions concerning the state-of-the-art in various electro-optical technologies and their potential applicability to the weapon delivery problem. Paper studies and standardization studies were initiated by different organizations within the Air Force in response to some of the questions raised (Ref 22:4-220).

This thesis topic was suggested by ASD/ENAMB as a result of an action item from this conference (Ref 22:4-218). This action item includes the requirement to ". . . decide (the) feasibility, desirability and applicability of pursuing new (electro-optical) development."

Organization

Section II establishes the Air Force requirements for the next generation electro-optical weapon system. The expected battlefield scenario is investigated and related operational constraints are defined.

Also, the specific comparison parameters are established along with their associated utility functions. These individual utility functions are then combined into an overall expression used for generating one figure of merit for each of the systems considered.

Sections III, IV and V present the theoretical and/or measured performance relative to the comparison parameters for the Nd:YAG, CO₂, and millimeter wave systems, respectively.

Section VI contains the results of the trade-off analysis using the requirements model developed in Section II and the data from Sections III, IV and V.

Finally, the concluding remarks are made in Section VII, including observations and recommendations.

II Air Force Requirements

Scenario

The factor which most determines the requirements for the next generation electro-optical weapon system is the conditions under which it will be used. As stated previously in the Scope section, this thesis addresses the scenario where the Air Force must stop, or, at the very least, slow, an armored ground assault against the United States or one of her allies. Although an analysis of the current world situation is not offered in this study, it is assumed that the most probable source of such an assault is the Soviet Union or another Warsaw Pact country and that the target of the attack is a NATO alliance country. Specifically, it is assumed that the country under attack is West Germany and that the offensive movements originate from East Germany where the greatest majority of the military personnel and equipment are Soviet and where the tactics are totally Soviet. This means that the attacking forces consist primarily of tanks with a smaller percentage of armored personnel carriers (APCs) and self-propelled antiaircraft vehicles. A brief description of some of these potential targets is given in Table I. A general deployment concept is shown in Figure 1 depicting the type of Soviet organization which might be used in the assumed attack scenario. Using this format as a guide, the relative numbers of vehicles are given in Tables II and III as a function of the distance behind the FEBA (Forward Engagement Battle Area). Based upon this proposed engagement scenario, the two primary tactical targets for the defending Air Force are the T-72 tank and the ZSU-23/4 mobile antiaircraft vehicle shown in Figures 2 and 3, respectively. For the

Table 1
Potential Soviet Target (Ref 14:38)

Type	Designation	Characteristics
AAA	SA-8	Self-contained, wheeled Acquisition/tracking radar Manual TV target acquisition Four radar guided missiles
	ZSU-23/4	Self-propelled Acquisition/tracking radar Optical sight Four 23 mm machine guns Firing range of 2.5 km
Tanks	T-72	125 mm main gun/auto loader Coaligned 7.62 mm machine gun 12.7 mm AA machine gun Smoke laying capability
	T-62	Low silhouette 115 mm main gun Coaligned 7.62 mm machine gun 12.7 mm AA machine gun

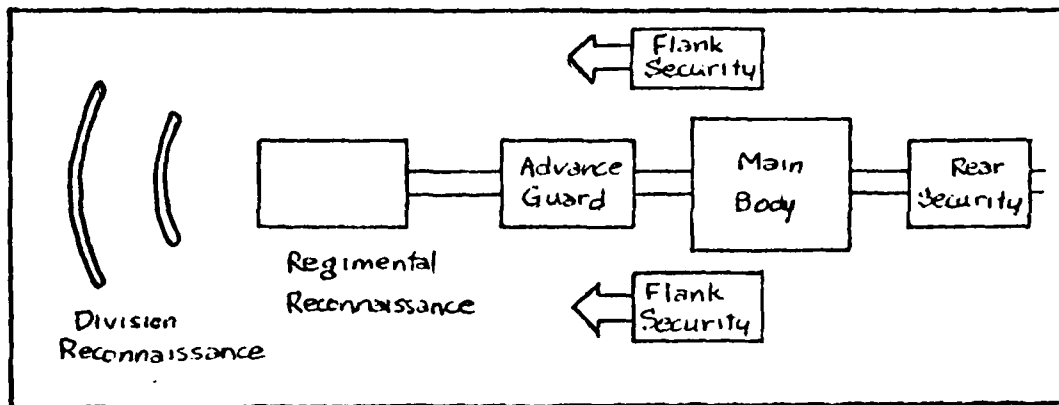


Figure 1. Typical Soviet Deployment Concept (Ref 14:46)

Table II

Soviet Target Distribution (Ref 14:44)

Distance from FEBA	Tanks	APC's	Artillery	AAA
0-20 km	478	242	186	112
20-40 km	282	173	91	52
40-60 km	189	196	117	45
60-80 km	207	257	130	36
80-100 km	-	-	-	12

Table III

Distribution of Key Air Defenses (Ref 14:44)

Distance from FEBA	SA-8	ZSU-23/4
0-20 km	40	32
20-40 km	14	12
40-60 km	12	10
60-80 km	10	10
80-100 km	4	-

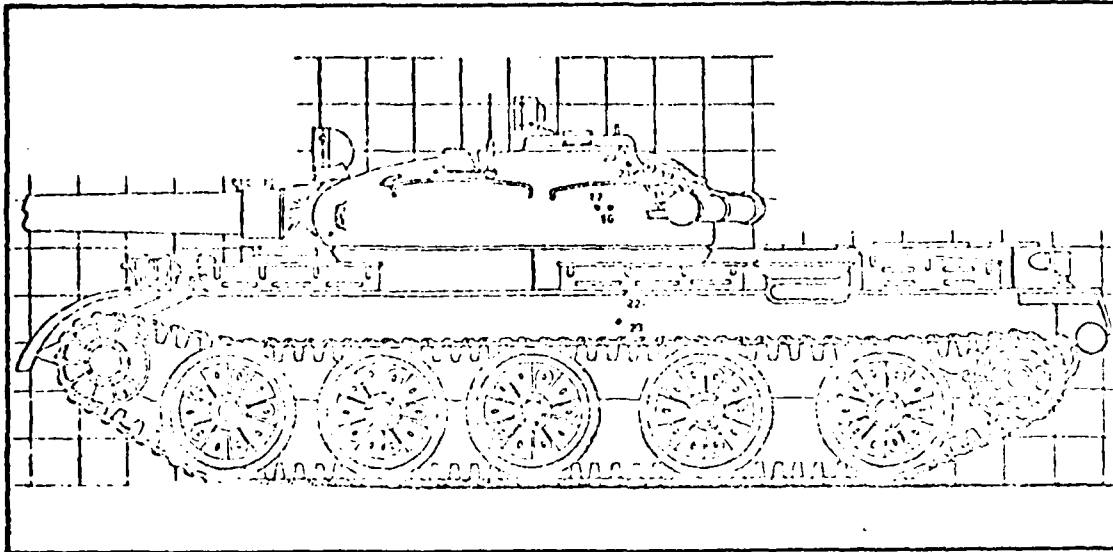


Figure 2. Soviet T-72 Tank (Ref 3)

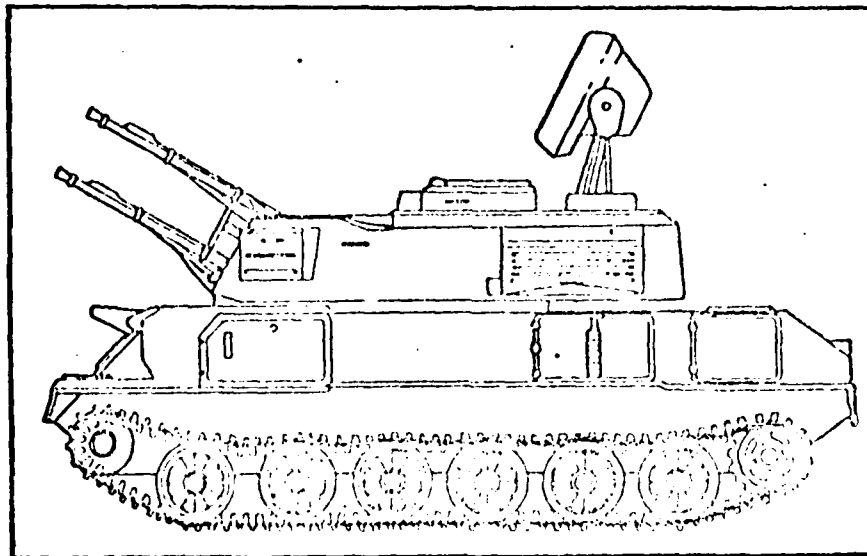


Figure 3. Soviet ZSU-23/4 Mobile Anti-Aircraft Vehicle (Ref 3)

purposes of this study, however, these primary targets are represented, geometrically, by a 10 foot by 20 foot rectangle positioned perpendicular to the aircraft-to-target line of sight. While this is not intended to represent the worst case which would be a front aspect view of the target, it is intended to provide a target compatible with quarter views, side views and down looking views.

The attacking aircraft is required to fly at very low altitudes to avoid the enemy anti-aircraft artillery (AAA). Both the A-10 and F-16 are considered as the airborne platforms for the next-generation electro-optical weapon system (Ref 18). Where individual requirements differ between the two aircraft, the worst case condition is used to define system requirements. An approach altitude of 50 meters above ground level (AGL) is used for all calculations as this is considered a reasonable compromise between aircraft safety from enemy AAA and ground obstacles while still providing sufficient range for target detection (Ref 3;14;15;18). This scenario is schematically depicted in Figure 4.

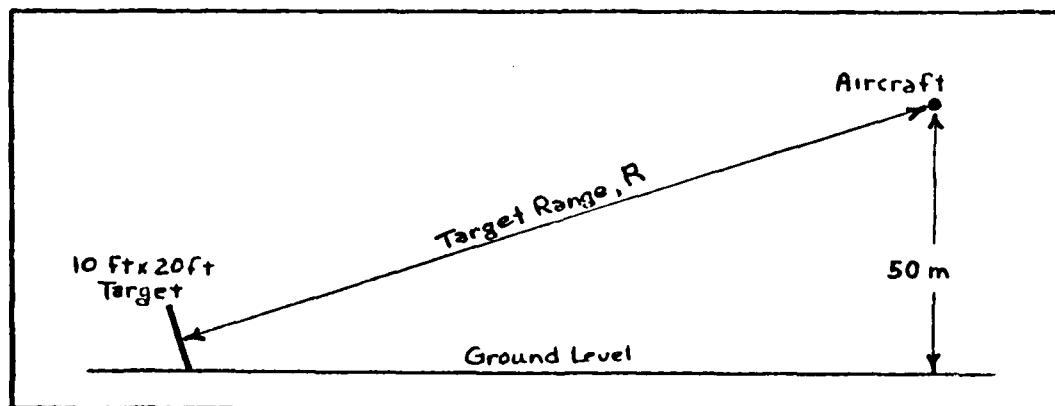


Figure 4. Attack Suppression Scenario

Since the central European area is considered to be a probable area of engagement, and since current electro-optical weapon systems are greatly affected by weather conditions, several studies have been conducted in order to characterize the atmospherics of the East Germany/West Germany border area (Refs 1:8:14:17). These studies have dealt, not only with optical visibilities, but also with cloud cover, fog characteristics and precipitation conditions. As this thesis considers only low altitude sorties, cloud cover effects on weapon system performance are not discussed. Also, since the probability of rainfall occurring is small, shown in Figure 5, precipitation effects are not considered. This restriction is valid when considering probable mobility degradations to the enemy during rain conditions.

Fog, on the other hand, is a relatively frequent atmospheric occurrence in the area of concern, as shown in Figure 6, and is generally characterized as an atmospheric condition with a visibility less than or equal to 1 kilometer. Figure 7 shows that, given the occurrence of fog, degraded visibility can last several hours. This thesis, therefore, uses fog as a definition for degraded atmospheric transmission. Individual fog effects on various wavelengths are presented later in their appropriate sections.

When natural obscurants such as fog do not exist during an enemy attack, it is assumed that visual cover will be generated by the deployment of smoke. Several types of smoke are used by the allied countries and assumed to be used by the Warsaw Pact countries. Some of the more common smokes are white phosphorus (WP), plasticized white phosphorus (PWP), red phosphorus (RP),

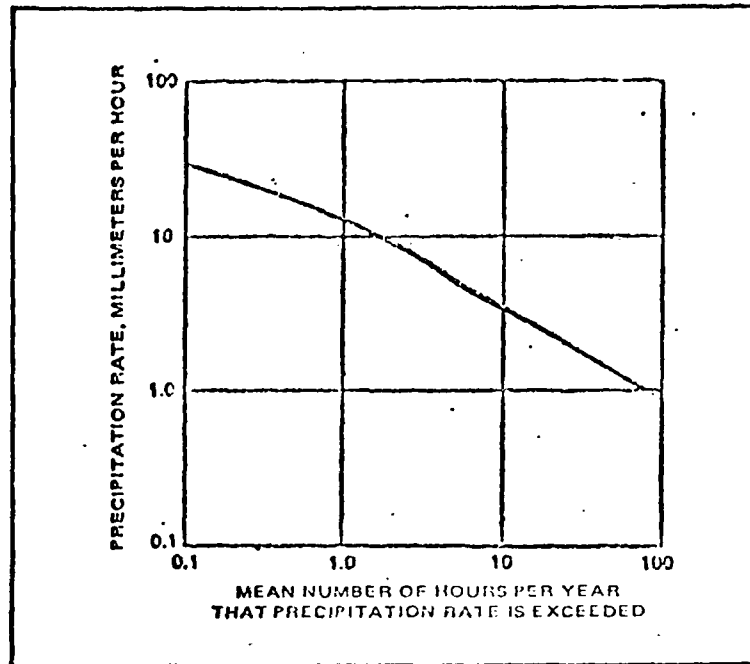


Figure 5. Mean Number of Hours per Year Precipitation Rate is Exceeded (Ref 14:26)

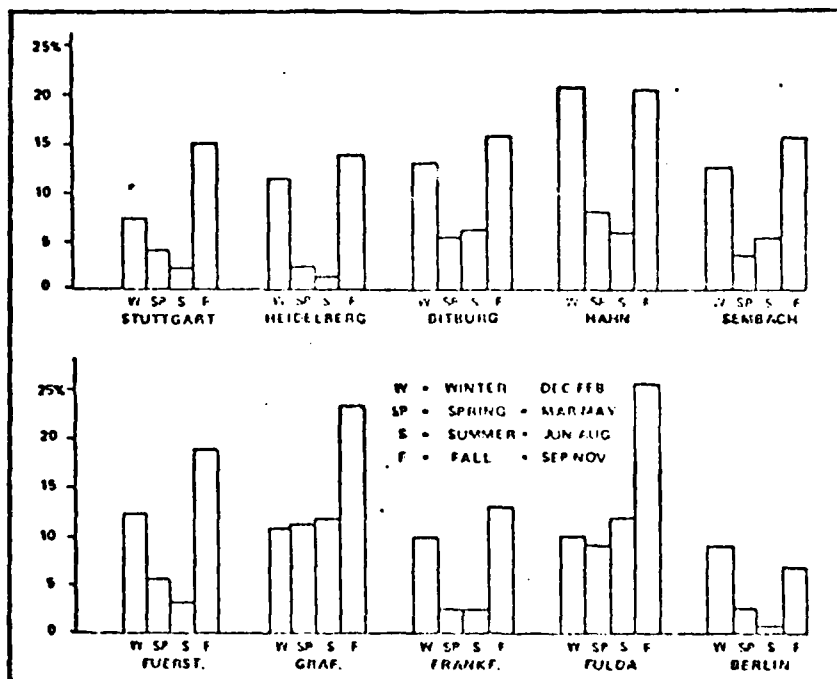


Figure 6. Frequency of Fog (Ref 8:3)

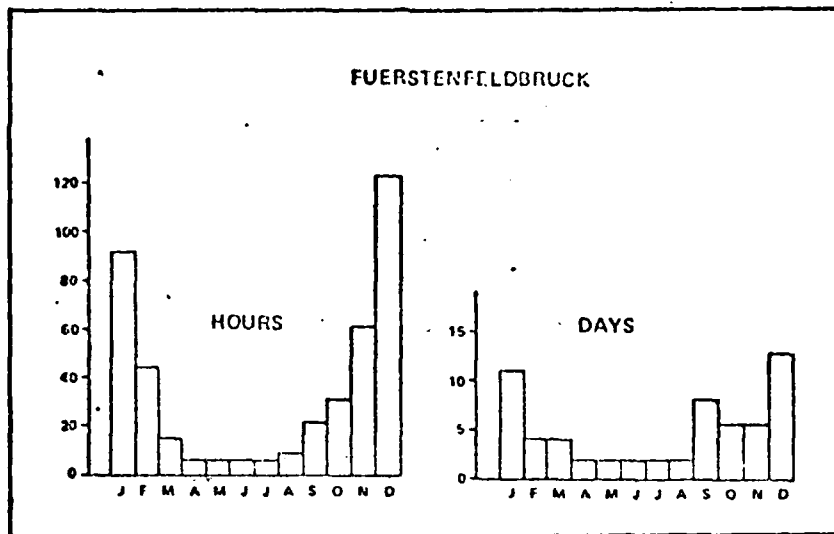


Figure 7. Maximum Duration of Fog (Visibility \leq 1 km) (Ref 8:3)

hydrogen chloride (HC) and fog oil aerosol (Ref 25). These smokes can be generated either by smudge pots which are placed in position and then ignited or by mortar or artillery shelling (Ref 25). The geometry of the resulting smoke cloud depends on several factors, but most strongly on the wind direction and speed. For purposes of calculations in this thesis, it is assumed that the horizontal extent of the smoke cloud is approximately 100 feet (or about 30 meters) in front of the enemy target and that its concentration is 0.1 g/cu m. The vertical extent of the smoke cloud is assumed to be great enough to cause the target-to-aircraft line-of-sight to penetrate the entire 30 meters of smoke (Ref 23). This scenario is depicted in Figure 8. This thesis

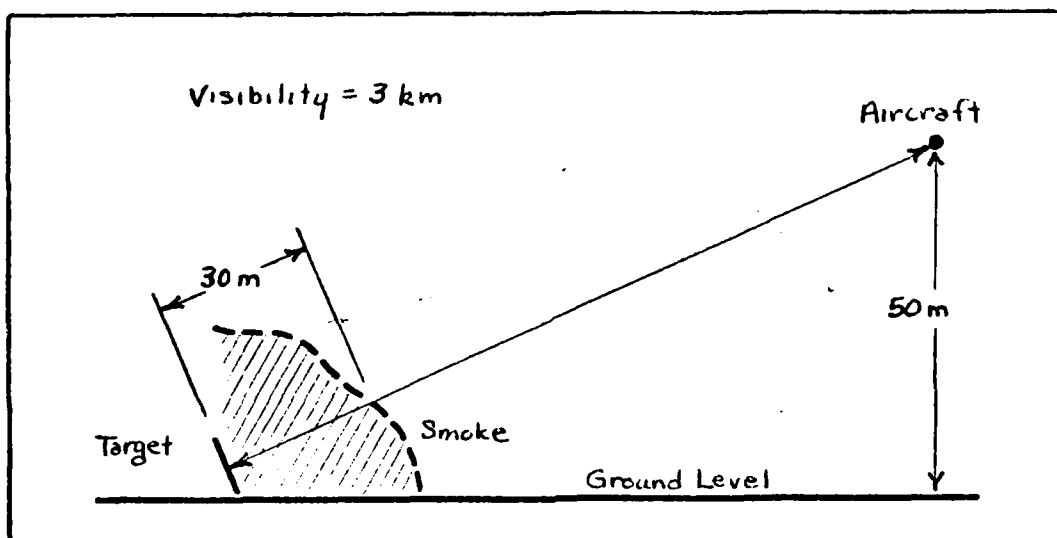


Figure 8. Smoke Scenario

uses the optical characteristics of white phosphorus for the smoke scenario calculations. This smoke is very common and, as can be seen in Figure 9, has high effectivity in the visual spectrum. It is also assumed that the atmospheric visibility when the smoke is deployed is that of haze (approximately 3 km).

The actual attenuation mechanisms and methods of calculation for both atmospherics and smokes are contained in the following sections for the specific wavelengths.

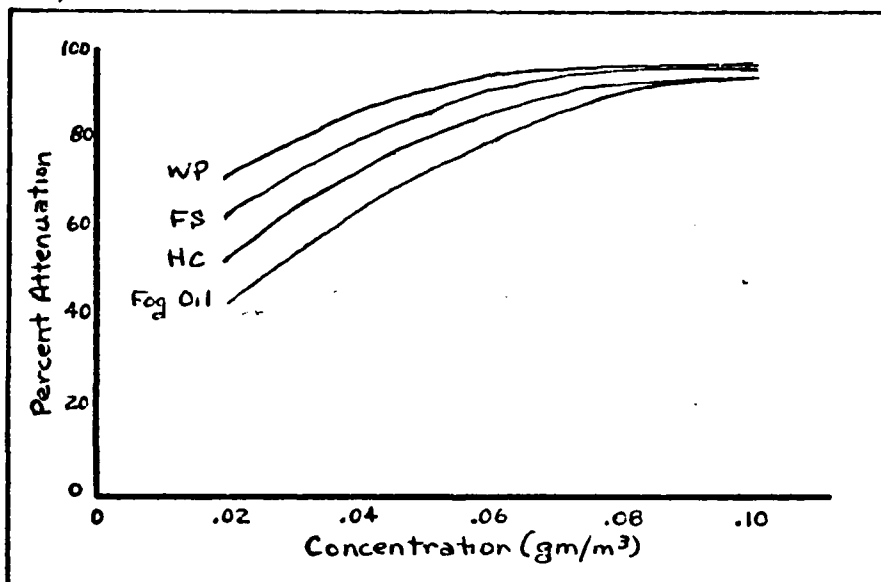


Figure 9. Visual Attenuation Through Various Smokes (Ref 14:34)

Defining Critical Parameters

In selecting one weapon system over another, several factors can, and should, be considered. These factors include overall system performance, maintainability, reliability, cost and its possible initial operational capability (IOC) date among many others. The one person, or group of people, who is responsible for this decision must perform some sort of a trade-off analysis, whether consciously through a

structured trade-off study, or unconsciously by mentally weighting the various parameters. Either route can produce a mass of seemingly unrelated numbers describing numerous advantages or disadvantages of the competing systems. A final decision is, therefore, sometimes difficult to come to and even more difficult, in some cases, to justify. This thesis attempts to perform the trade-off analysis contained herein using a method which quantifies the choices and makes the decision process a matter of comparing one figure of merit for each candidate system.

The method used is one discussed by Keeney and Raiffa (Ref 16) dealing with decision making given multiple objectives and multiple inputs. This approach is currently used in the business community as a way of optimizing decisions to achieve the best possible capital investment (Ref 12). The first step in this method is to define the critical system parameters which have the greatest value to the decision maker in the projected utility of the system. For each of the parameters, a value function is generated which establishes a relationship between the particular parameter and an associated numerical rating (ranging from 0 to 1). This is generally accomplished in an interview with the decision maker by asking his rating on specific numbers within the range of the parameter in question. A value of "0" is given to the least desirable number for the parameter and a "1" given to the most desirable number. The remainder of the function is then found by systematically identifying parametric values with their associated numerical rating.

One person in the Air Force who closely exemplifies the type of decision maker necessary for the selection of the next generation electro-optical weapon system is Dr. Bernard Kulp, Chief Scientist for the United States Air Force Systems Command. In an interview with Dr. Kulp (Ref 18), several characteristics of weapon systems were discussed as to their relative importance to the required trade-off analysis. Among those parameters discussed were:

1. Lock-on ranges in various scenarios.
2. Physical characteristics of the weapon system such as weight and exterior dimensions.
3. Weapon delivery accuracy.
4. Electrical interface between the weapon system and the aircraft.
5. System reliability.
6. System maintainability.
7. Approximate IOC (Initial Operational Capability) date.
8. Cost associated with both the development and the production of the weapon system.

It is recognized that a system's overall utility can be severely limited by any of the above characteristics. In order to limit the analysis to a manageable level, however, the following rationale is used (Ref 18). Since this trade-off analysis investigates candidate systems at their current state-of-the-art performance, development and production costs associated with advancing the state-of-the-art are not applicable, thereby reducing a large part of the cost uncertainty. It is assumed, therefore, that the cost of adding

the next generation E-0 weapon system to the Air Force inventory will be approximately constant for the individual candidates. The IOC date is not considered to be critical since the typical time to bring a new weapon system into the inventory is at least five years. Again, since state-of-the-art advancements are not considered necessary, schedule uncertainties are reduced, thereby allowing the assumption that the development and production schedules will be similar for the various candidates. Also, since the results of this thesis are to be used to support a decision for the engineering development for a weapon system, design dependent characteristics such as reliability, maintainability and electrical interface represent areas which would be addressed during the design phase of the system. As such, these parameters are not appropriate when investigating wavelength inherent performance characteristics. Of the parameters remaining, the following are considered by Dr. Kulp to be the most critical:

1. Penetration of tactically deployed smokes.
2. Atmospheric penetration with visibilities < 3 miles.
3. CEP (Circular Error Probability) of the weapon.
4. Diameter of the aircraft-mounted pod.

The rationale for the first two is directly attributable to the scenario description given previously. The importance of the CEP is logical since it directly affects target destruction. The wavelength dependence of the CEP is developed later in this section as is the impact of the pod diameter on system performance. The utility functions for each of these parameters are discussed below.

Smoke

The smoke penetration requirement is driven by aircraft survivability in the AAA scenario discussed previously. For this reason, the parameter used to indicate system smoke penetration is the system's detection range in the specified smoke scenario. Figure 10 shows the detection range utility function in the smoke environment. The data is from both results of the questioning procedure described earlier (Ref 3) and from general perceptions of the ranges required (Refs 15 and 18). A mathematical approximation to this data is developed using the general form:

$$U(R_{sm}) = A \{ 1 - \exp [\alpha (R_{sm} - \beta)] \} \quad (1)$$

where β shifts the curve horizontally to the proper location,

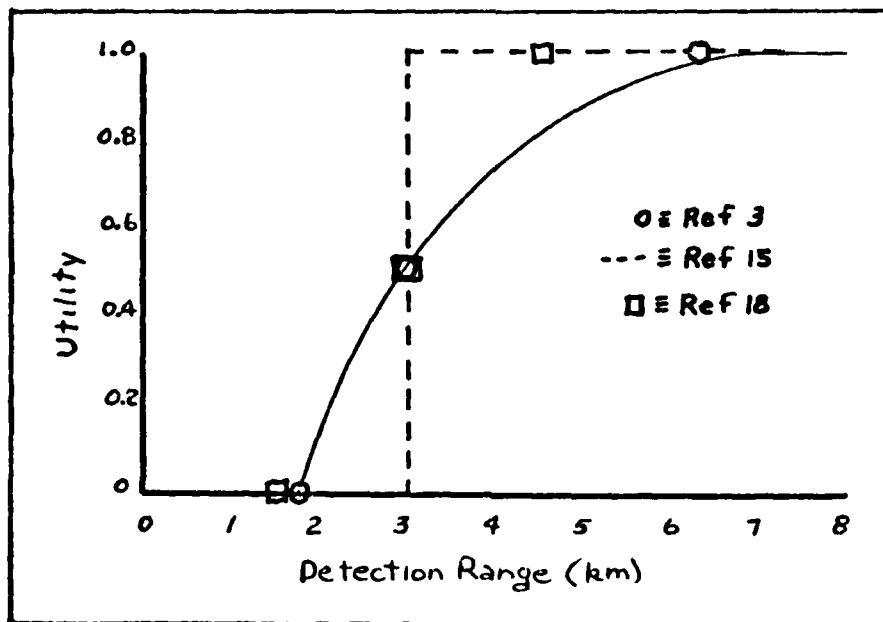


Figure 10. Utility Function for Smoke Scenario

α defines the rate of increase in the resulting exponential curve and A essentially normalizes the curve to a utility of 1.0 for the appropriate value of R_{sm} . The reason for selecting the exponential function are two-fold. First of all, it provides a reasonable fit to the available data. Secondly, it has a constant risk aversion defined by

$$r(x) = - \frac{u''(x)}{u'(x)}$$

where

$r(x)$ = risk aversion at the parameter value x

$u''(x)$ = second derivative of the utility function at x

$u'(x)$ = first derivative of the utility function at x

Having a decreasing or constant risk aversion means that, as x increases, the decision maker's inclination to risk a reduction in the parameter value when faced with the opportunity of increasing it decreases or remains constant. In other words, the larger the x value, the incremental loss of utility associated with an incremental reduction of the parameter value is not increased. This is an appropriate model for the decision maker in the Air Force since he is rarely more willing to take a chance at improving performance when the possible loss is greater. Based upon the data in Figure 10, the following points can be used to find the model:

$$U(6.5) = 1.0 \tag{2}$$

$$U(3.0) = 0.5 \tag{3}$$

$$U(1.8) = 0.0 \tag{4}$$

The values from Equations (2), (3) and (4) are then substituted into Equation (1) to determine the values of A, α and β to be 1.04, -0.62 and 1.8, respectively. Equation (1) then becomes

$$U_1 (R_{sm}) = 1.04 \{ 1 - \exp [-0.62 (R_{sm} - 1.8)] \} \quad (5)$$

The validity of Equation (5) is shown in Figure 10 where it is compared with the actual data.

Weather

The weather penetration requirement for the Air Force is driven, as in smoke, by the desirable target detection range. It can be assumed, therefore, that an applicable model for weather penetration is one identical to that generated for the smoke environment. This model is defined by Equation (6):

$$U_2 (R_{wx}) = 1.04 \{ 1 - \exp [-0.62 (R_{wx} - 1.8)] \} \quad (6)$$

The model curve in Figure 10 is, therefore, identical for the adverse weather scenario and is not repeated here.

CEP

The CEP of a weapon system is a total system accuracy parameter which statistically combines several performance factors such as designator pointing stability, inherent missile accuracy and spot size of illuminating energy on the target. The utility function for CEP is converted to a spot size utility function so as to segregate as much as possible the wavelength dependent performance factors from other system design related parameters. This conversion is performed

by starting with an approximate utility function for the probability of hit based on various sources providing general concepts on the format of the curve (Refs 3, 6 and 18) for an armor piercing weapon. This function is shown in Figure 11. Assuming that the system miss distance is normally distributed with the CEP defined as the 1σ value, the relationship between CEP and probability of hit is shown in Figure 12. Figure 11 can then be expressed in terms of CEP and is presented in Figure 13.

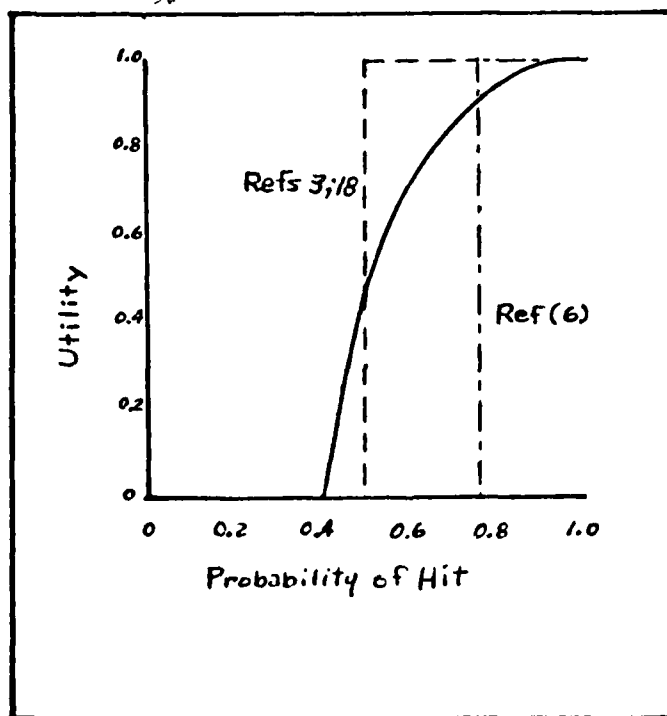


Figure 11. Utility Function for Probability of Hit

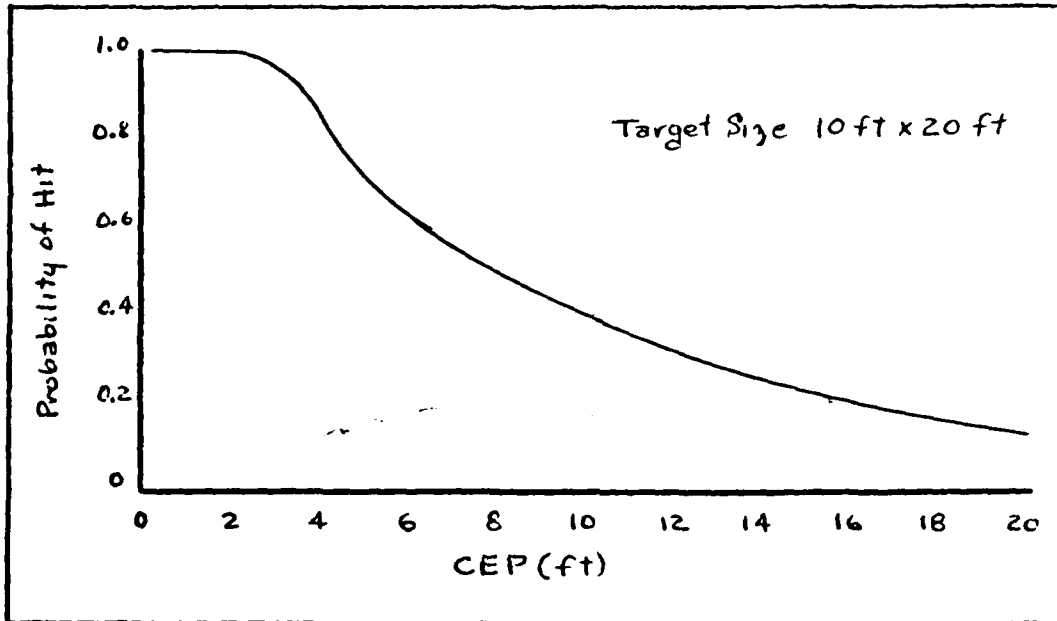


Figure 12. Relationship Between CEP and Probability of Hit (Ref 6)

In order to separate spot size from the overall system CEP, it is necessary to establish their interrelationship. While this relationship is extremely intricate and depends significantly on various characteristics of the specific guided weapon being considered and on the launch geometry, it can be simplified by making the following assumptions. First, it is assumed that the weapon miss distance (CEP) tracki g a stationary point target is Gaussian distributed with a typical 1σ value of 1.22 m for precision anti-tank air-to-ground guided

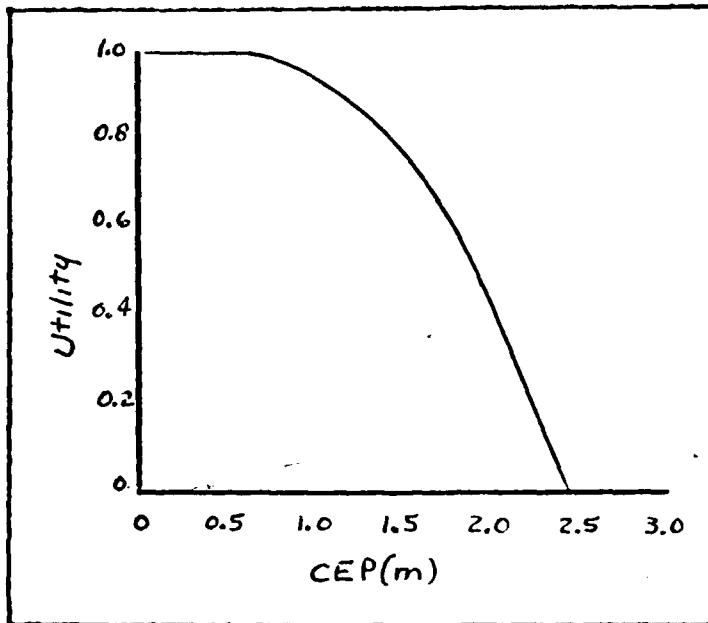


Figure 13. Utility Function for CEP

missiles (Ref 6). Secondly, it is assumed that the spot wander on the target (spot jitter) is minimized by some sort of closed-loop pointing and tracking control. If the spot jitter can be maintained at $50 \mu\text{rad}$ (1σ value), a stand-off range of 6 km results in a 0.3 m 1σ spot jitter on the target. Furthermore, it is assumed that the energy cross section of the designator beam is Gaussian distributed and that the probability of the weapon tracking a particular point within the target spot follows a Gaussian distribution centered about the highest level of the energy distribution. The overall weapon system CEP can then be expressed as in Equation (7):

$$\sigma_{cep}^2 = \sigma_s^2 + \sigma_j^2 + \sigma_w^2 \quad (7)$$

where

σ_{cep} = Total weapon system CEP

σ_s = Spot size (1 σ of energy distribution)

σ_j = Spot jitter on target

σ_w = Weapon miss distance against a stationary point target

Solving for the spot size, Equation (7) becomes

$$\sigma_s = (\sigma_{cep}^2 - \sigma_j^2 - \sigma_w^2)^{1/2} \quad (8)$$

Substituting the typical values for spot jitter and missile miss distance given above, Equation (8) becomes

$$\sigma_s = (\sigma_{cep}^2 - 1.58)^{1/2} \quad (9)$$

The utility function for spot size can then be found by using Figure 13 in conjunction with Equation (9). The resulting curve is shown in Figure 14. The corresponding model uses the form of Equation (1) and the following points from Figure 14:

$$U(0.0) = 1.0 \quad (10)$$

$$U(1.0) = 0.8 \quad (11)$$

$$U(2.2) = 0.0 \quad (12)$$

The values for A, α and β are found to be 1.10, 1.08 and 2.2, respectively, resulting in Equation (13):

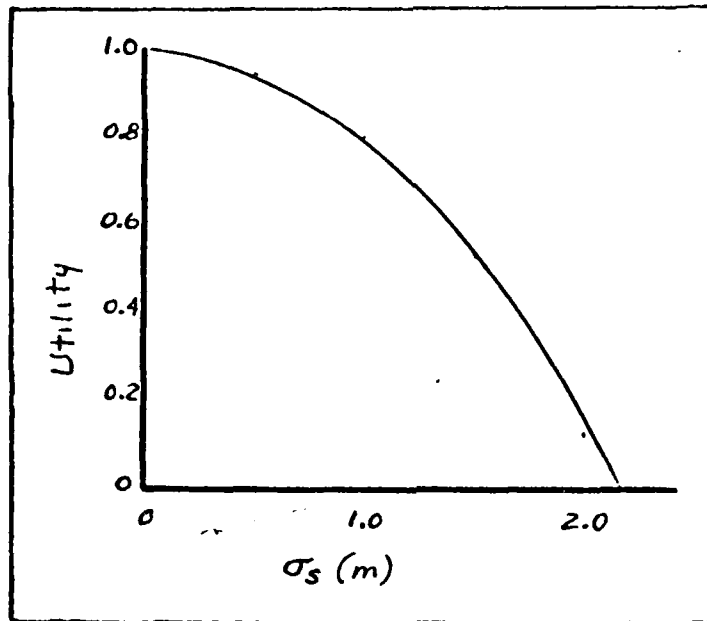


Figure 14. Utility Function for Spot Size

$$U_3 (\sigma_s) = 1.10 \{ 1 - \exp [1.08 (\sigma_s - 2.2)] \} \quad (13)$$

Pod Diameter

The two major considerations for the required pod diameter are the resulting aerodynamic loading on the aircraft and the mechanical interface with the aircraft. Based on computer simulation of pod diameter impact on the F-16 performance shown in Figure 15, and on discussions with Mr. Roger Brislawn (Ref 5), the limiting factor on the diameter of the pod is its mechanical interface with the aircraft. This results from the proposed location of the next

generation electro-optical pod being the side inlet of the F-16 shown in Figure 16. At this location, a diameter larger than 15 inches interferes with an access panel on the intake scoop and would necessitate moving the pod to one of the wing stations. This move would result in the replacement of a weapon or an auxiliary fuel tank, making such a move highly undesirable. The utility function in Figure 17 reflects these constraints with a sharp decline near 15 inches. Again, Equation (1) is used to find the required model. Using the values of

$$U(0) = 1.0 \quad (14)$$

$$U(10) = 0.95 \quad (15)$$

$$U(15) = 0 \quad (16)$$

from Figure 17, the values for A, α and β are found to be 1.00, 0.60 and 15.0, respectively. The resulting model is

$$U_4(D) = 1 - \exp [0.60 (D - 15.0)] \quad (17)$$

System Utility Function

To develop an overall system utility function model, the four preceding models for the individual parameters of interest must be combined. A good approximation to this system function is found by assuming that the individual parameters are mutually pairwise independent. Although it is recognized that in the strict sense, this assumption is violated in this case, as in the example of R_{sm} and R_{wx} , the

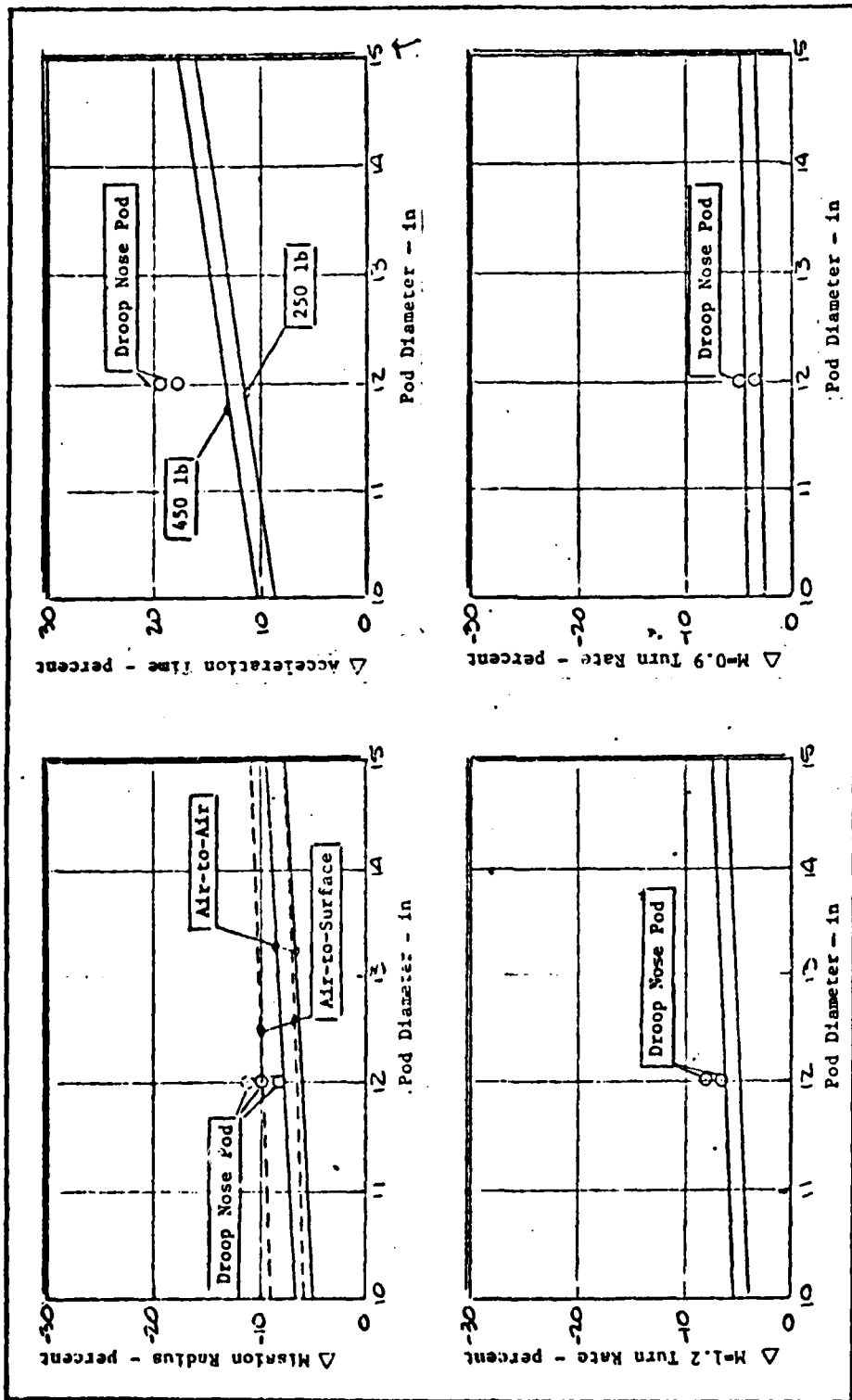


FIGURE 15. POD SIZE AND WEIGHT IMPACTS F-16 AIRCRAFT PERFORMANCE

SIDE INLET AND CENTERLINE LOCATION (Ref 9:107)

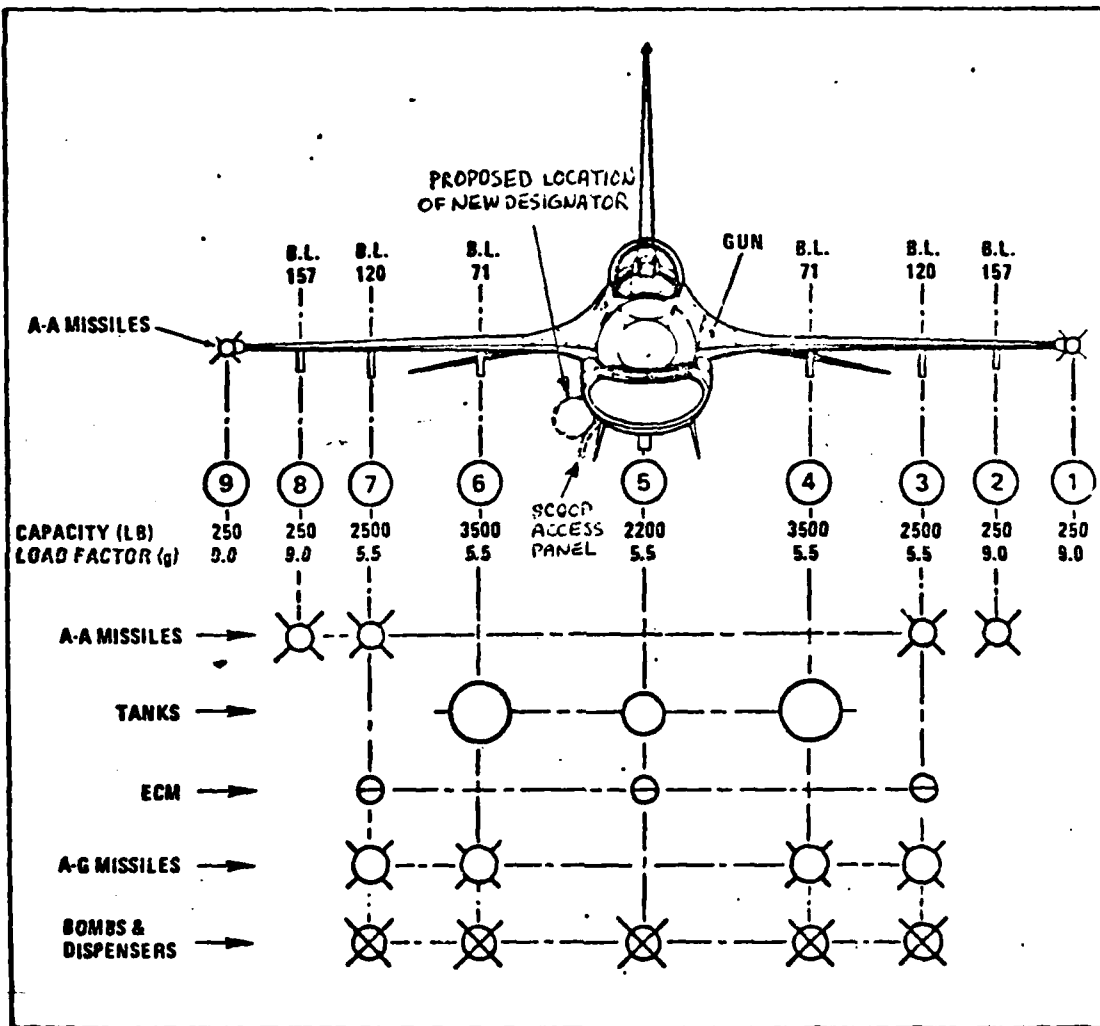


Figure 16. F-16 External Store Capability (Ref 9:109)

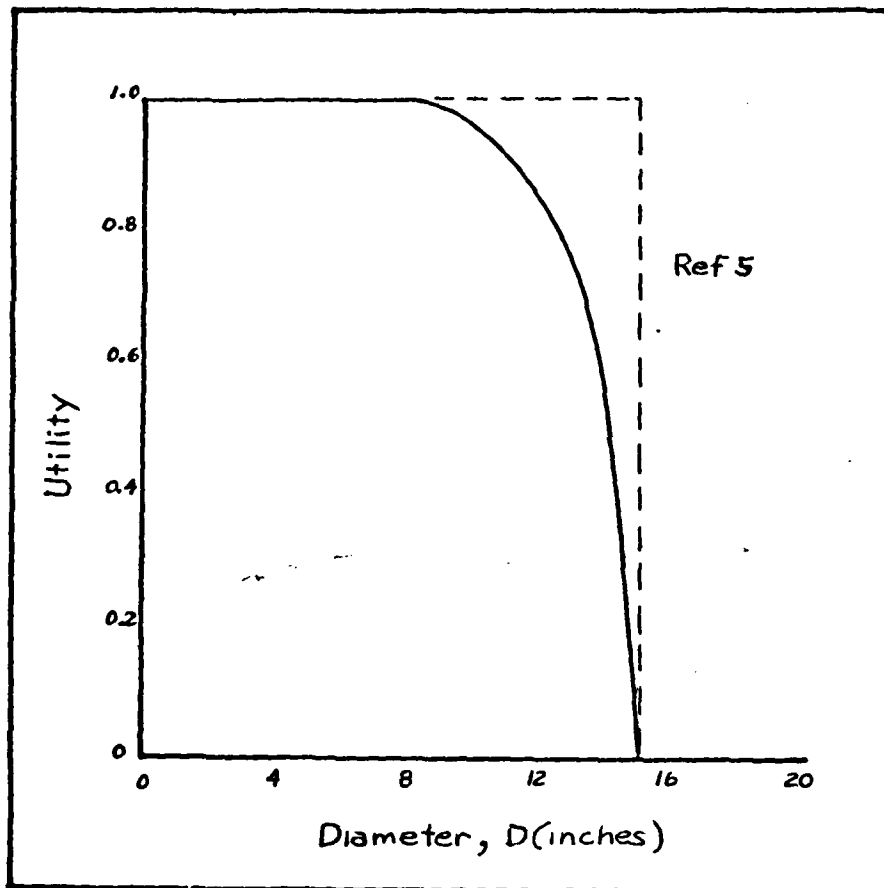


Figure 17. Utility Function for Pod Diameter

resulting model still provides usable information on the relative utilities of various systems. The independence assumption allows the overall system utility function to be

expressed as a weighted sum of the individual utility functions developed previously, i.e.

$$U (R_{sm}, R_{wx}, \sigma_s, D) = \sum_{i=1}^4 \lambda_i U_i \quad (18)$$

The functions U_1 , U_2 , U_3 , and U_4 are defined by Equations (5), (6), (13) and (17), respectively, while the values for λ must be determined by the following method. First, it is known that since

$$U_1(1.8) = U_2 (1.8) = U_3 (2.2) = U_4 (15.0) = 0 \quad (19)$$

$$U (1.8, 1.8, 2.2, 15.0) = 0 \quad (20)$$

Also, since

$$U_1(7.0) = U_2 (7.0) = U_3 (0.0) = U_4 (8.0) = 1 \quad (21)$$

$$U (7.0, 7.0, 0.0, 8.0) = \sum_{i=1}^4 \lambda_i \quad (22)$$

By definition, the greatest system utility occurs when each of the parametric utility functions have values of 1.0 (as in Equations (21) and (22)) and is also equal to 1.0, therefore

$$\sum_{i=1}^4 \lambda_i = 1 \quad (23)$$

To define the values of the λ coefficients, general interrelationships are used based on conversations with several different sources (Refs 5; 6; 7; 11; 15; 18; and 23). The relative order of priority is R_{sm} , R_{wx} , σ_s and D . All minimum values of the respective utility

functions are initially used as in Equation (20). One parameter of the system utility function is increased to its maximum value and then equated; in terms of utility, to a lesser increase in a higher priority parameter. This procedure is shown below for the comparison of R_{sm} and R_{wx} :

$$\begin{aligned} U(R_{sm} = 1.8, R_{wx} = 7.0, \sigma_s = 2.2, D = 15.0) \\ = U(R_{sm} = 5.0, R_{wx} = 1.8, \sigma_s = 2.2, D = 15.0) \end{aligned}$$

or, from Equation (18),

$$\begin{aligned} \lambda_1 U_1(1.8) + \lambda_2 U_2(7.0) + \lambda_3 U_3(2.2) + \lambda_4 U_4(15.0) \\ = \lambda_1 U_1(5.0) + \lambda_2 U_2(1.8) + \lambda_3 U_3(2.2) + \lambda_4 U_4(15.0) \end{aligned}$$

Using Equations (19) and (21), this reduces to

$$\lambda_2 = \lambda_1 U_1(5.0)$$

From Figure 10

$$U_1(5.0) = 0.90$$

therefore

$$\lambda_2 = \lambda_1 (0.90) \tag{24}$$

This method is then applied to comparing R_{wx} to σ_s and σ_s to D below:

$$U(1.8, 1.8, 0.0, 15.0) = U(1.8, 5.0, 2.2, 15.0)$$

$$\lambda_3 = \lambda_2 U_2(5.0)$$

$$\lambda_3 = \lambda_2(0.90) \quad (25)$$

$$U(1.8, 1.8, 2.2, 8.0) = U(1.8, 1.8, 1.5, 15.0)$$

$$\lambda_4 = \lambda_3 U_3(1.5)$$

$$\lambda_4 = \lambda_3(0.58) \quad (26)$$

By combining Equations (23), (24), (25) and (26) the values for the λ coefficients are found to be

$$\lambda_1 = 0.31$$

$$\lambda_2 = 0.28$$

$$\lambda_3 = 0.26$$

$$\lambda_4 = 0.15$$

Equations (5), (6), (13), (17) and (27) are then substituted into Equation (18) to form the overall weapon system utility function

$$\begin{aligned}
U (R_{sm}, R_{wx}, \sigma_s, D) = & 1.00 - 0.31 \exp [- 0.62 (R_{sm} - 1.8)] \\
& - 0.28 \exp [- 0.62 (R_{wx} - 1.8)] \\
& - 0.26 \exp [1.08 (\sigma_s - 2.2)] \\
& - 0.15 \exp [0.60 (D - 15.0)]
\end{aligned}
\tag{28}$$

This model is now used to determine one figure of merit, the numerical utility, for each of the systems considered.

III Nd:YAG Designator System

Weather Penetration

The standard propagation equation for a laser designator is given in Equation (29) (Ref 2:9):

$$P_r = \left(\frac{P_t}{R^2 \Omega_t} \right) (\rho A_r) \left(\frac{A_c}{R^2 \Omega_r} \right) T^2 \quad (29)$$

where

P_r = received power

P_t = transmitted power

ρ = target reflectivity

A_r = target area

A_c = receiver clear aperture area

Ω_t = transmit solid angle beamwidth

Ω_r = target solid angle scattered beamwidth

T = one-way propagation path transmittance

By assuming that all of the transmitted energy is incident on the target, i.e. $A_r \geq R^2 \Omega_t$, Equation (29) can be reduced to

$$P_r = \frac{P_t \rho A_c}{R^2 \Omega_r} T^2$$

Also, assuming that the target reflectance is diffuse and, therefore, Lambertian

$$\Omega_r = 2 \pi$$

and

$$P_r = \frac{P_t \rho A_c}{2 \pi R^2} T^2$$

where

$$T^2 = \exp [-2 \sigma R]$$

where σ represents the propagation medium attenuation in km^{-1} .

Equation (29) can then be written as

$$P_r = \frac{P_t \rho A_c}{2 \pi R^2} \exp [-2 \sigma R] \quad (30)$$

The minimum detectable power is derived by first establishing a required single hit probability of detection (assume $P_D = 90\%$) and a required false alarm rate (assume 1 false alarm/minute). Using radar detection theory, the false alarm rate is used to calculate a false alarm number, n , (Ref 20:21) by

$$n = B N t_{fa} \quad (31)$$

where

B = electrical bandwidth of receiver

N = number of pulses integrated

t_{fa} = false alarm time = (false alarm rate)⁻¹

By assuming the bandwidth is approximately 10 MHz (Ref 1:IV-8) and that N must be one for the single hit case, n is found to be approximately 2×10^9 . This value, in conjunction with $P_D = 90\%$, is then used to define the required signal to noise ratio (SNR). Utilizing the Swerling Case 2 radar target model which is applicable for specular reflections (Ref 1:IV-3), the required SNR is found in the appropriate Meyer plot (Ref 20:335), a variation of which is shown in Figure 18, to be 23 db. The detectivity, D^* , for a representative silicon p-n junction detector is found from the appropriate curve in Figure 19 to be 4×10^{12} cm Hz^{1/2}/W. Noise equivalent power (NEP) is then computed from the relationship

$$NEP = \frac{A_d B}{D^*} \quad (32)$$

where

A_d = detector active area

B = bandwidth of noise

D^* = normalized detectivity

Assuming a detector active area of 5.0 cm^2 (approximately 1 inch in diameter) and the bandwidth remaining at 10 MHz, the NEP for this detector (and the $1.06 \text{ }\mu\text{m}$ system) is 1.77×10^{-9} watts, which, for an SNR of 23 db, results in $P_r = 3.53 \times 10^{-7}$ watts.

The atmospheric attenuation coefficient, σ , depends on the specific weather conditions specified. As stated previously, the presence of fog is assumed with an optical visibility less than 1000 m. It is unrealistic, however, to define an adverse weather scenario severe enough to restrict aircraft flight. A realistic fog scenario is presented in Figure 20 which requires fog penetration of 100 m one-way with the remainder of the line-of-sight in a moderate to thick haze. For these calculations, the optical visibility of the haze is defined as 3 km (Ref 24:7-8) while 400 m visibility is used for fog. The particular type of fog used for this thesis is a radiation fog based on the relative probability of occurrence shown in Figures 21 and 22. Corresponding attenuation coefficients for the haze and fog conditions are listed in Table IV. Nominal values for the remaining parameters in Equation (30) are (Refs 1; 2; 6; 14)

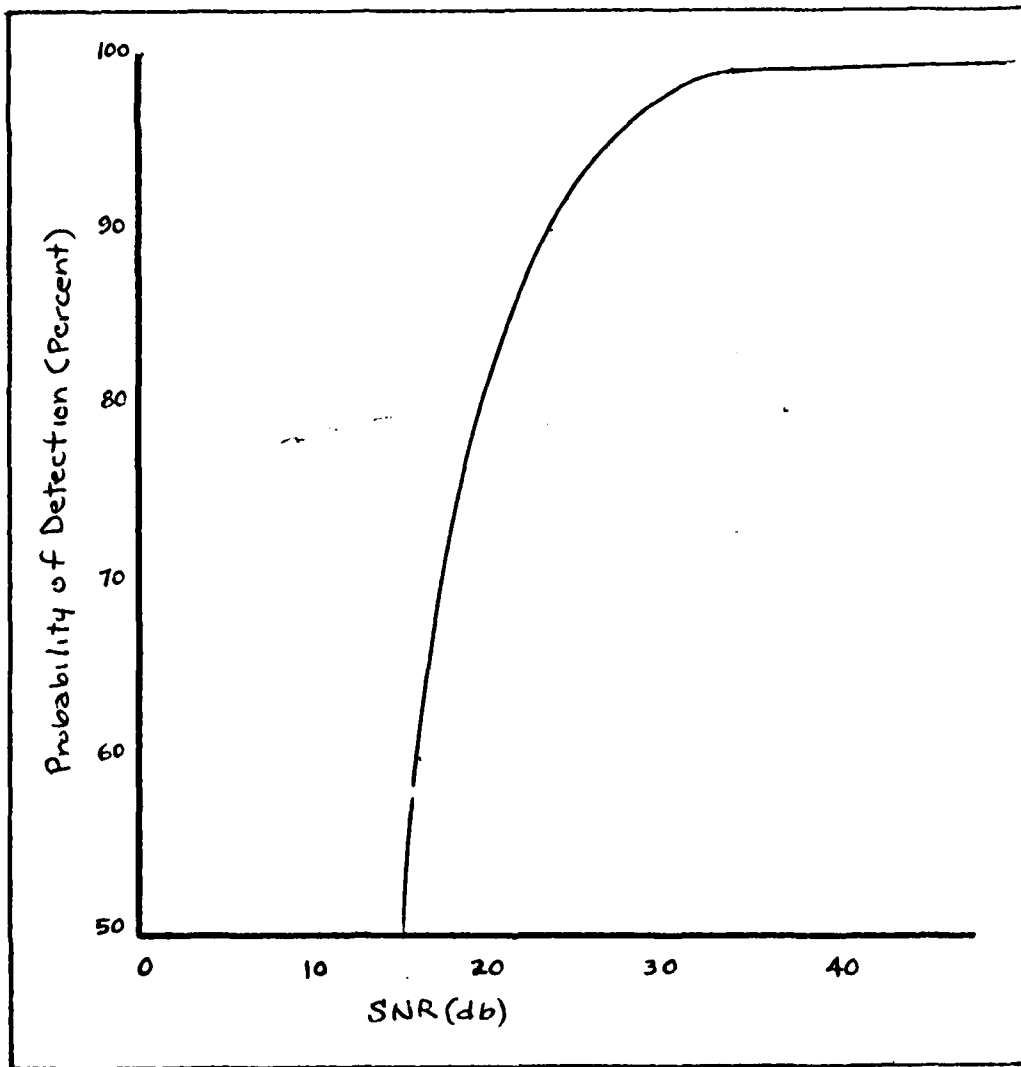


Figure 18. Probability of Detection vs SNR for $n = 2 \times 10^9$
and $N=1$

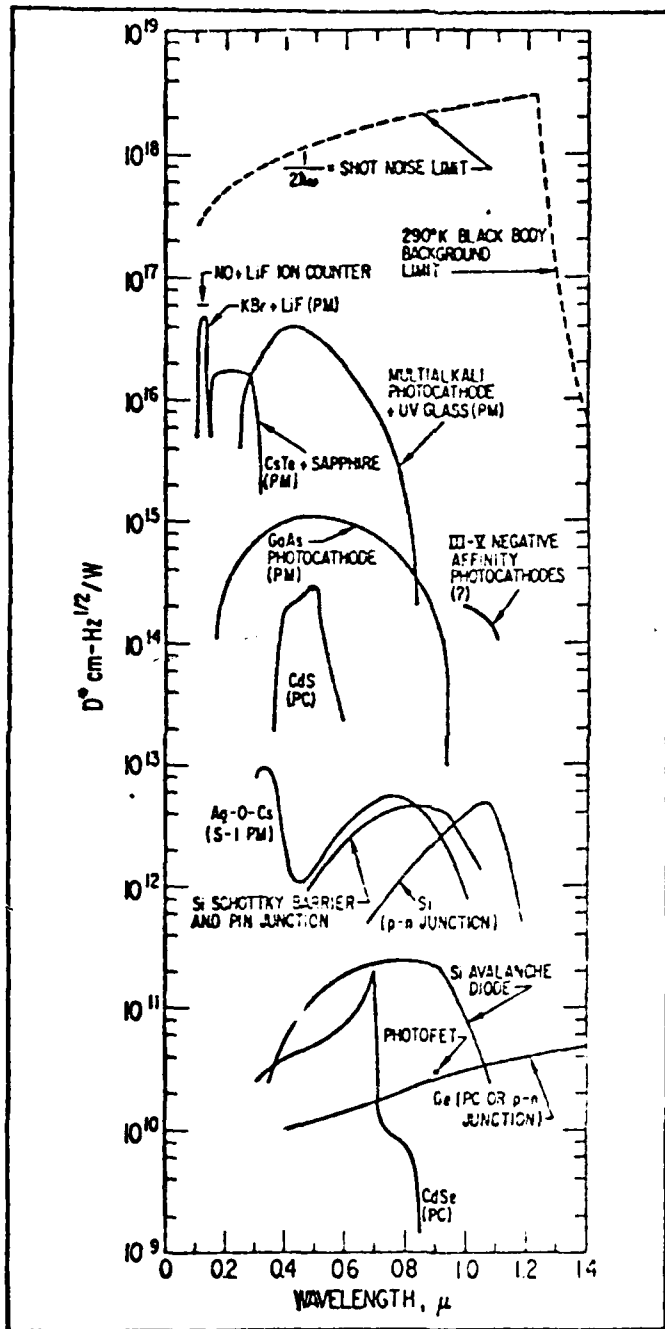


Figure 19. Typical Detectivities for Various Near Infrared Detectors (Ref 13)

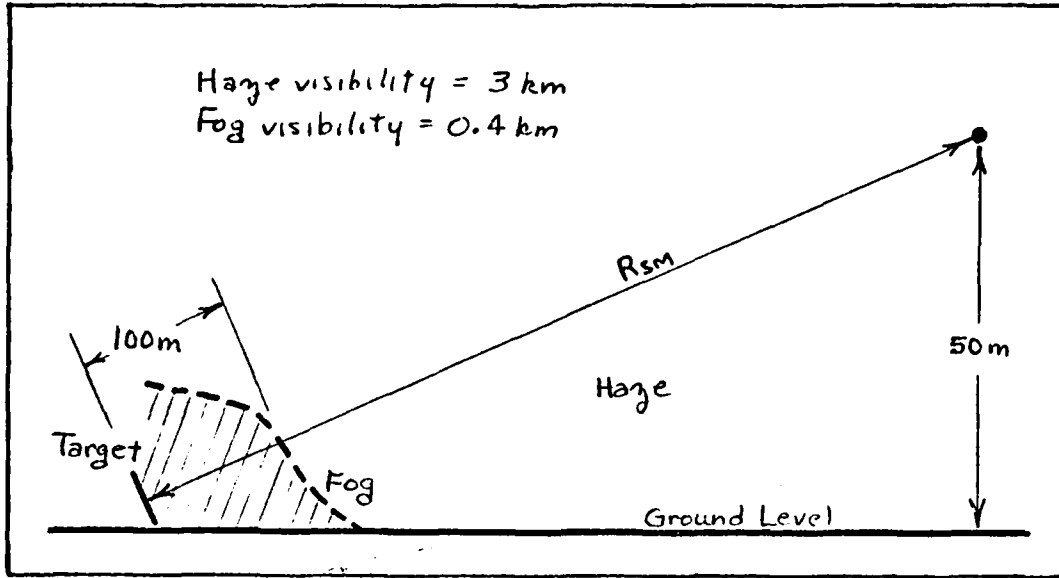


Figure 20. Fog/Haze Scenario

Table IV

Atmospheric Attenuation Coefficients for 1.06 μm

Weather Condition	Visibility	Attenuation Coefficient (km^{-1})
Haze	3.0	0.88 (Ref24:7-8)
Radiation Fog	0.4	9.78 (Ref17:32)

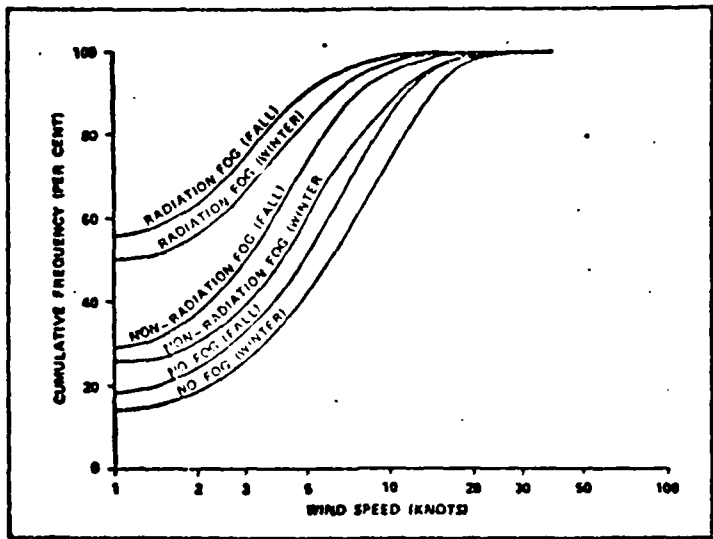


Figure 21. Wind Speed vs Probability of Occurrence (Ref 8)

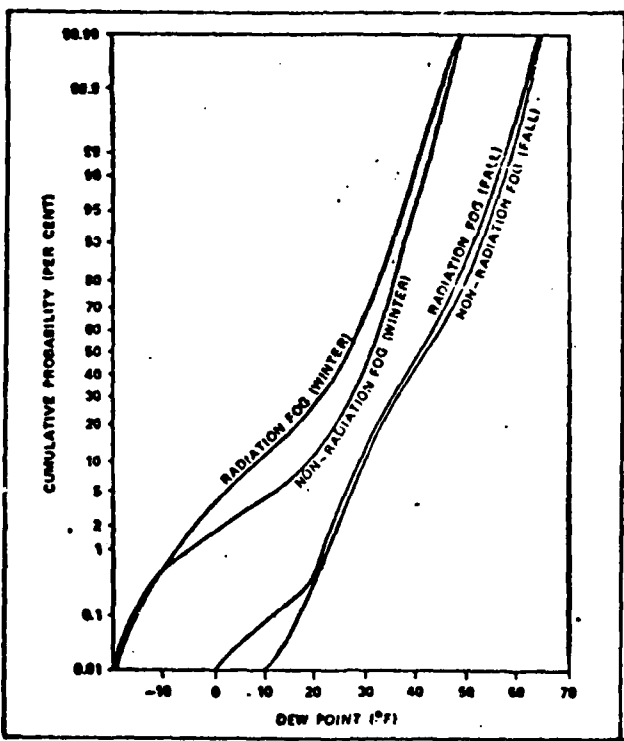


Figure 22. Dew Point vs Probability of Occurrence (Ref 8)

$$p = 0.1$$

$$P_t = 10^7 \text{ watts}$$

$$A_c = 50 \text{ cm}^2 \text{ (Approximately a 3 inch diameter)}$$

Equation (30) can now be rewritten to include these values and to reflect the weather scenario of Figure 20 as

$$R_{WX} = \left(\frac{P_t \rho A_c}{2\pi Pr} \right)^{1/2} \exp [-0.1 (\sigma_f - \sigma_h)] \exp [-\sigma_h R_{WX}] \quad (33)$$

or

$$R_{WX} = 19.50 \exp [-0.88 R_{WX}] \quad (34)$$

which, when solved iteratively, results in

$$R_{WX} = 2.38 \text{ km} \quad (35)$$

Smoke Penetration

The calculation of smoke penetration follows precisely the format used for weather penetration. The only changes required are the replacement of the fog attenuation coefficient with an appropriate smoke attenuation coefficient, σ_{sm} , and the replacement of the 100 m thick fog model with the 30 m thick smoke model. A value used for the smoke attenuation coefficient is found to be $1 \text{ m}^2/\text{g}$ for $1.06 \mu\text{m}$ radiation in white phosphorus smoke. When combined with the previously assumed smoke concentration of $0.1 \text{ g}/\text{m}^3$ gives an attenuation coefficient of 100 km^{-1} . Equation (33) then becomes

$$R_{sm} = \left(\frac{P_t \rho A_c}{2\pi P_r} \right)^{1/2} \exp [-0.03 (\sigma_{sm} - \sigma_h)] \exp [-\sigma_h R_{sm}] \quad (36)$$

Equation (36) assumes, as in the case for weather penetration, that the atmospheric visibility outside of the smoke is approximately 3 km (haze). Substituting the above values into Equation (36) gives

$$R_{sm} = 2.43 \exp [-0.88 R_{sm}]$$

which results in

$$R_{sm} = 1.01 \text{ km} \quad (37)$$

Spot Size

Spot size is calculated based upon the assumption that beam divergence results from Fraunhofer diffraction at the Nd:YAG laser exit port. Setting the exit port diameter at 1 cm, Equation (38) can be used to find the beam divergence:

$$\theta = \frac{1.22 \lambda}{d} \quad (38)$$

where

θ = beam divergence (full width)

λ = wavelength

d = exit port diameter

A value of 0.13 mrad results from this equation. The actual spot

size depends on the actual aircraft to target range and is found by $\sigma_s = \Theta R$ to be 0.13 m for $R_{sm} = 1.01$ km and 0.31 m for $R_{wx} = 2.38$ km. Since the weapon system must satisfy both the adverse weather and smoke requirements, the limiting condition on the spot size for the Nd:YAG system is

$$\sigma_s = 0.15 \text{ m} \quad (39)$$

Pod Diameter

The external dimensions for the type of weapon system pod addressed in this thesis are affected by the types of functions it is expected to perform. The driving factor on its size can either be the electro-optical device and its associated optics or it can be the required processing electronics. Systems currently in the Air Force inventory demonstrate that the limiting factor on the pod diameter is not the Nd:YAG laser or its associated detection optics, but instead the optical requirements for a collocated imaging system. Examples of this are found in the Pave Spike system (TV camera) with a diameter of 8-12 inches and the Pave Tack system (FLIR) with a 12-14 inch diameter. For purposes of this trade-off analysis, therefore, the aircraft mounted pod diameter for a Nd:YAG system is estimated to be

$$D = 12 \text{ inches} \quad (40)$$

IV CO₂ Designation System

Weather Penetration

The CO₂ system weather penetration performance is calculated using the same methods as in Section III. A required probability of detection of 90% and a false alarm rate of 1/min results in a required SNR of 23 db. The noise equivalent power, however, is changed based upon a different detectivity for the 10.6 μm case. From Figure 23, D* for a Hg_(1-x)Cd_xTe (mercury cadmium telluride) is approximately 10¹⁰ cm Hz^{1/2}/watt. Utilizing Equation (32) with the same values for the bandwidth and detector active area as for the Nd:YAG system, the NEP for the CO₂ system is found to be 7.07 X 10⁻⁷ watts. For a SNR of 23 db, the received power, therefore, must be 1.41 X 10⁻⁴ watts.

Attenuation coefficients for 10.6 μm radiation are presented in Table V. These values are then used in Equation (33) to find R_{wx}.

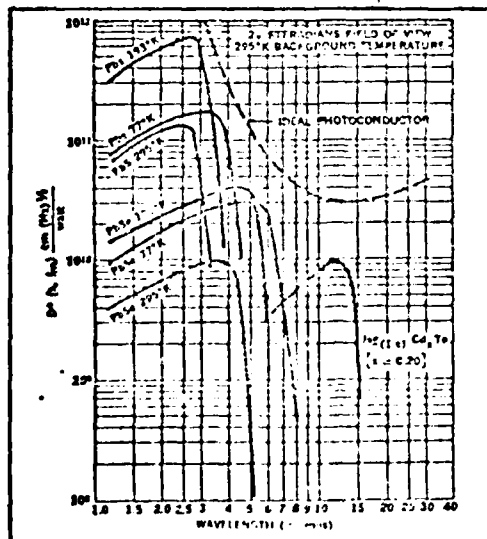


Figure 23. Detectivities for Infrared Sensors (Ref 13)

Table V

Atmospheric Attenuation Coefficients for 10.6 μm

Weather Condition	Visibility (km)	Attenuation Coefficient (km^{-1})
Haze	3.0	0.65 (Ref 17 :32)
Radiation Fog	0.4	1.96 (Ref 17 :32)

The 1.06 μm case values are used for ρ and A_r while a representative transmitter power, P_{T1} of 4 kilowatts is used (Ref 1:V-6).

Equation (33) then becomes

$$R_{wx} = 0.04 \exp [-0.65 R_{wx}]$$

which results in a value of $R_{wx} = 0.039 \text{ km}$. If a heterodyne detector is used in place of the direct detection method, however, the system NEP can be represented by (Ref 2:16)

$$\text{NEP} = \frac{h\nu}{\eta t} \tag{41}$$

where

h = Planck's constant = 6.626×10^{-34} joules - sec

ν = frequency of radiation = 2.83×10^{13} Hz

η = quantum efficiency = 0.50 (Ref 26 :14)

t = pulse duration = 20 nsec

Equation (41) results in a NEP of 1.87×10^{-12} watts and a minimum

$P_r = 3.73 \times 10^{-10}$ watts for a SNR of 23 db. Equation (33) then becomes

$$R_{wx} = 25.63 \exp [-0.65 R_{wx}]$$

which results in

$$R_{wx} = 3.20 \text{ km} \quad (42)$$

Smoke Penetration

Equation (36) is used for the smoke penetration calculation with a value of $0.4 \text{ m}^2/\text{g}$ for the mass extinction coefficient (Ref 25:81). Combining this value with the assumed concentration of 0.1 g/m^3 gives $\sigma_{sm} = 40 \text{ km}^{-1}$. The equation then becomes

$$R_{sm} = 8.97 \exp [-0.65 R_{sm}]$$

which provides

$$R_{sm} = 2.17 \text{ km} \quad (43)$$

Spot Size

Using Equation (38), the spot sizes corresponding to R_{wx} and R_{sm} are 4.14 m and 2.81 m, respectively. Again, selecting the limiting case leaves

$$\sigma_s = 2.07 \text{ m} \quad (44)$$

Pod Diameter

The same limiting situations discussed for the diameter

of Nd:YAG systems previously are assumed to be applicable to the CO₂ system. In fact, conceptual design studies have been conducted on the feasibility of a CO₂ laser radar resulting in a proposed external pod diameter of 10 inches (Ref 1:V-15). For this trade-off analysis, therefore, the CO₂ pod diameter is

$$D = 10 \text{ inches} \quad (45)$$

V Millimeter Wave Designation System

Weather Penetration

By using Equation (38) to take a quick look at the spot size of a millimeter wave system, it is noted that even for the least desirable pod diameter, 15 inches, being equated to the exit port of the device, beam divergence is 10.21 mrad. At the typical ranges being considered in this thesis, 10.21 mrad causes a spot size of at least 20 m in diameter. It cannot be assumed, therefore, that all of the transmitted energy is incident on the 10 foot by 20 foot target.

The SNR analysis for a probability of detection of 90% and a false alarm rate of 1/min is still valid, however, and a value of 23 db is still used. The determination of the NEP is slightly different drawing on radar theory for the 94 GHz system.

Equation (46) defines the radar NEP (Ref 20:6)

$$NEP = kTB\overline{NF} \quad (46)$$

where

$$k = \text{Boltzmann's constant} = 1.381 \times 10^{-23} \frac{\text{joule}}{\text{molecule} \cdot \text{°k}}$$

$$T = \text{temperature (°k)}$$

$$B = \text{system bandwidth}$$

$$\overline{NF} = \text{noise factor}$$

Typical values for these parameters are (Ref 26)

$$T = 290^{\circ}\text{K}$$

$$B = 10 \text{ MHz}$$

$$\bar{N}\bar{F} = 10$$

These values result in a NEP = 4.00×10^{-13} watts for a $P_r = 7.98 \times 10^{-11}$ watts. This number can then be used in the radar range equation

(Ref 10 :74)

$$P_r = \frac{P_t G_t G_r \lambda^2 \sigma}{(4\pi)^3 R^4} \exp [-2 \alpha R] \quad (47)$$

where

G_t = gain of transmitting antenna

G_r = gain of receiving antenna

λ = wavelength

σ = radar target cross section

P_t = power transmitted

P_r = power received

α = atmospheric attenuation coefficient

R = target to radar range

The relationship between gain and the antenna is given by

$$G = \frac{4 \pi \eta A}{\lambda^2} \quad (48)$$

where

η = efficiency factor = 0.55 typically (Ref 23)

A = effective antenna aperture

For the millimeter wave system, it is assumed that the transmitting antenna is also the receiving antenna. This is a standard design procedure for radar systems where two large antennas can be replaced by one dual function antenna. Also, even though it is recognized that the missile's receiver antenna cannot be as large as the pod's and, therefore, cannot match the pod's detection range, it is assumed that the missile could be designed to lock-on after launch. This prevents the missile's receiver from limiting overall system performance. It can then be stated that $G_t = G_r$ so that Equation (47) can be solved for R to become

$$R = \left(\frac{P_t \sigma \eta^2 A^2}{4 \pi P_r \lambda^2} \right)^{1/4} \exp \left[- \frac{\alpha R}{2} \right] \quad (49)$$

The appropriate attenuation coefficients are given in Table VI for 94 GHz radiation.

Table VI
Atmospheric Attenuation Coefficients for 94 GHz

Weather Condition	Visibility (km)	Attenuation Coefficient (km ⁻¹)
Haze	3.0	0.21 (Ref 26)
Radiation Fog	0.4	0.23 (Ref 26)

A value of 15 inches is assumed for the antenna diameter and, therefore, an aperture of 0.11 m^2 . A nominal transmitter power for a 94 GHz radar is 1 kwatt peak power (Ref 26). Equation (49) can then be written as

$$R_w = 24.37 \sigma^{1/4} \exp \left[-\frac{0.1}{2} (\sigma_f - \sigma_h) \right] \exp \left[-\frac{\sigma_h R_{wx}}{2} \right]$$

or

$$R_{wx} = 24.35 \sigma^{1/4} \exp \left[-0.10 R_{wx} \right]$$

Since the incident beam is expected to spill over onto the terrain surrounding the target, the terrain's reflectance is used to calculate the radar cross section. The projected ground coverage of the radar is

$$A_{gc} = \frac{\pi}{A} \theta^2 R^2$$

Using a reflectivity of 0.1 (Ref 10:98)

$$\sigma = .1 \frac{\pi}{4} \theta^2 R^2 = 8.19 R^2$$

where R is in km. The range equation then becomes

$$R_{wx} = 1696.84 \exp \left[-0.20 R_{wx} \right]$$

which results in

$$R_{wx} = 21.78 \text{ km} \tag{50}$$

Smoke Penetration

Recent smoke tests conducted utilizing 94 GHz radars show that the presence of the types of smoke discussed earlier have no detectable effect on atmospheric transmission for the 94 GHz radar (Ref 4:2-9). Given this fact, the smoke range can be written as

$$R_{sm} = \frac{P_t \sigma \eta^2 A^2}{4 \pi P_r \lambda^2}^{1/4} \exp \left[- \frac{\sigma_h}{2} R_{sm} \right]$$

which results in

$$R_{sm} = 24.37 \sigma^{1/4} \exp \left[- 0.10 R_{sm} \right]$$

or

$$R_{sm} = 21.79 \text{ km} \quad (51)$$

It must be noted at this point that lock-on ranges would be significantly decreased if the missile's receiver required a majority of the incident energy to fall on the target. In the case described above, the intended target is actually a small section of the illuminated area. The resulting degradation to the overall system utility is addressed later.

Spot Size

In the 94 GHz case, the spot size can again be determined by Equation (38) resulting in a spot size of

$$\sigma_s = 111.24 \text{ m}$$

Pod Diameter

Since the antenna diameter is considered to be the limiting factor, the 94 GHz radar diameter is

$$D = 15 \text{ inches} \quad (52)$$

VI Results

The values for R_{wx} , R_{sm} , σ_s , and D from Sections III, IV and V are now used in the overall utility model of Equation (28) to obtain the individual utilities of the systems under consideration. These results are shown in Table VII.

Table VII
Utility Values for Candidate System

System	R_{sm} (km)	R_{wx} (km)	σ_s (m)	D (in)	Utility
Nd:YAG	1.01	2.38	0.15	12	0.25
CO ₂	2.17	3.20	2.07	10	0.40
MMW	21.79	21.78	111.24	15	-10 ⁵⁰

These utilities represent the expected benefit to the Air Force from using the candidate wavelength systems for point-tracking air-to-ground weapon system applications only. Any attempt to relate the results expressed in Table VII to different tactical applications, such as laser radar or beam rider weapon systems, is totally invalid since the overall system utility function for different applications will change drastically. These changes would include, not only differences in the inter-parameter relationships, but also the type and number of the parameters necessary to adequately state the Air Force requirement.

Table VII does show, however, that for the scenario outlined in this thesis, the most desirable wavelength is the $10.6\mu\text{m}$ CO_2 system, followed by the Nd:YAG system ($1.06\mu\text{m}$) and the millimeter wave system (94 GHz). The relative desirability of these systems is established, not by their performance advantages, but by their disadvantages. This is shown in Figure 24 where a performance value falling below the zero utility value actually accumulates a negative utility. Such a negative utility negates other positive attributes of the system, e.g., the poor spot size of the millimeter wave system completely overshadows the large lock-on ranges.

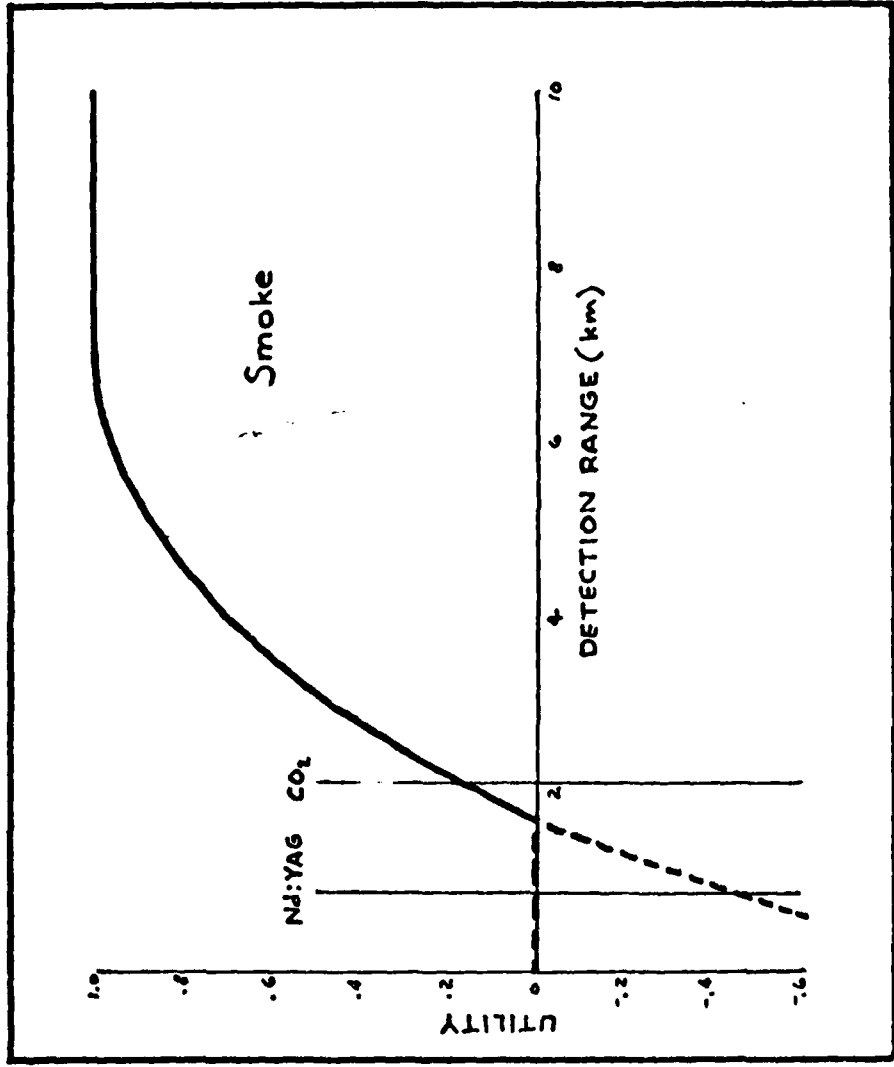


Figure 24. Example of Negative Utility

VII Conclusions

Observations

The main premise of this thesis is that the trade-off analysis of the various candidate wavelengths should be structured to reflect the specific requirements of the Air Force. In order to accomplish this, however, it is necessary to identify the decision baselines and, therefore, the decision maker. The ideal situation is to establish the value structures of the user of the end item. In the case of an air-to-ground tactical weapon in the Air Force, this user is the Tactical Air Command (TAC). It was difficult, however, to find in the active TAC wings the required understanding of parametric interrelationships necessary to formulate this type of decision model. In fact, the critical weapon system parameters were not defined until the discussions with Dr. Kulp of Systems Command. This fact identifies a gap, whether actual or apparent, between the system user and the system developer. Such a gap has the potential of creating severe inefficiencies in the development and deployment of new weapon systems. The decision method used in this thesis has a great potential of alleviating some of the inefficiency providing a developer decision model adequately reflects the user requirements. Even if this is the case, however, it must still be noted that the decision model only acts as an aid to quantify complex decisions by simulating some of the weighting processes performed mentally, either consciously or unconsciously, by the decision maker.

Another observation made is that in dealing with such a complex

decision problem as choosing the best weapon system, the decision model results depend strongly on the original limitations on the specific parameters used. This is seen in the fact that if, in this analysis, a larger effective CEP weapon is used, such as a guided bomb, the spot size limitation is relaxed. This would result in the superior detection range of the millimeter wave system giving it a higher utility than shown in Table VII.

It was also found that most people interviewed in an effort to define the utility functions had difficulty identifying parameter variation impact on its resulting utility. Their mental utility function is essentially a step function located at a parametric value identified with a specific requirement, as shown in the utility data in Section II. This limited view of system requirements can make everyday technical trade-offs a decision between white and black without considering grey. It can be seen from the values in Table VII that ignoring interparametric weighting and the utility function approach could place the millimeter wave system above the Nd:YAG and CO₂ systems.

Another observation was that a limit to the amount of negative utility achievable by any one parameter probably exists. This limit would have to be found as a negative extension to the utility curves using the same interview procedures described in Section II. Such a refinement would provide more realistic magnitudes for the overall system utility when one or more poor performance characteristics are encountered. The analysis conducted in this thesis, however, is detailed enough to establish the order of priority between the

candidate systems and, therefore, has met its stated objectives.

Recommendations

It is, first of all, recommended that a follow-on study be conducted to expand the utility model in an effort to encompass additional system considerations such as electrical interface, reliability, cost and weight. An analysis of background radiation and beam spill-over effects should also be conducted for the individual wavelengths to identify potential signal processing limitations.

It is also recommended that the resulting utility functions be programmed so as to determine the optimum achievable utility factor and its associated parameter values. These values can then be used as design goals for proposed plans of related hardware development.

Finally, a universal utility function could be developed which would contain a larger variety of electro-optical device tactical applications. These would include target designation (for small CEP weapons, large CEP weapons and beamriders), terrain avoidance, terrain following and obstacle avoidance. Such a function could be derived by first performing the analysis contained in this thesis for each tactical application. The results of these trade-off analyses could then be combined as are the individual parameters based on relative weightings and utility functions reflecting the Air Force requirements for the individual applications.

Bibliography

1. AFAL-TR-79-1163. CO₂ Laser Tactical Sensor Study. Hartford: United Technologies Research Center, October 1979.
2. Bachman, Christian G. Laser Radar Systems and Techniques. Dedham, Mass: Artech House, Inc., 1979.
3. Davies, Maj. R., Test Engineer for the A-10 SPO (personal interview). WPAFB, August 1980.
4. DRCPM-SMK-T-001-79. Smoke Week II. Electro-Optical (EO) Systems Performance in Characterized Obscured Environments at Eglin AFB, Florida. Eglin AFB: Department of the Air Force, March 1979.
5. Brislawn, Roger. Engineer for LANTIRN SPO (personal interview). WPAFB, 12 September 1980.
6. Eder, William. System performance engineer for the Maverick SPO (personal interview). WPAFB, 29 August 1980.
7. Elam, Tony. Electrical engineer, Pave Tack SPO (personal interview). WPAFB, 20 August 1980.
8. Essenwanger, O.M. and D.A. Stewart. Fog and Haze in Europe and Their Effects on Performance of Electro-Optical Systems. Report from US Army Missile Research and Development Command, Redstone Arsenal, Alabama.
9. FZM-6698. Preliminary Interface Specification F-16A to Advanced Laser Designator. General Dynamics, 12 December 1977.
10. Hall, W.M. "General Radar Equation", Radars Volume 2: The Radar Equation, edited by David K. Barton, Dedham, Mass., Artech House, Inc., 1977.
11. Hari, Lou. Electrical engineer, ASD/ENAMB (personal interview). WPAFB, 18 August 1980.
12. Hax, Arnolde C., Karl M. Wiig and Arthur D. Little, Inc. "The Use of Decision Analysis in Capital Investment Problems", Sloan Management Review, 17(2): 19-48 (Winter 1976).
13. Hengehold, Robert L. Lecture material distributed in PH 6.42, Optical Diagnostics Lab. School of Engineering, Air Force Institute of Technology, Wright-Patterson Air Force Base, 1980.
14. Hughes Aircraft Corporation. EOM Targeting Sensor Study. Avionics Lab Contract F33615-79-R-1803.

15. Huit, Maj. R. Engineer for TAC/DRA (personal interview). WPAFB, 7 August 1980.
16. Keeney, Ralph A. and Howard Raiffa. Decisions with Multiple Objectives: Preferences and Value Tradeoffs. New York: John Wiley & Sons, 1976.
17. Kneizys, F.X. et al. Atmospheric Transmittance/Radiance: Computer Code LOWTRAN 5. Report No. AFGL-TR-80-0067. Hanscom AFB, Mass., Air Force Geophysics Laboratory, 21 February 1980.
18. Kulp, B.A. Chief Scientist for USAF Systems Command (personal interview). Andrews AFB, 21 August 1980.
19. Lloyd, J.M. Thermal Imaging System. New York: Plenum Press, 1975.
20. Meyer, Daniel P. and Herbert A. Mayer. Radar Target Detection. New York and London: Academic Press, 1973.
21. Minutes of the USAF Armament and Avionics Planning Conference, 3 November 1978.
22. Minutes of the USAF Armament and Avionics Planning Conference, 15 October 1979.
23. Porubcansky, Tom. Avionics Lab smoke engineer (personal interview). WPAFB, 4 September 1980.
24. RCA Electro-Optics Handbook. Burlington, Mass., 1968.
25. Vervier, J.J. Smoke/Obscurant Technology. Chemical Systems Laboratory, Aberdeen Proving Ground, Maryland. Presented at the sixteenth IRIS Symposium on Infrared Countermeasures, 406 April 1978.
26. Wasky, Ray. Radar engineer for Avionics Laboratory (personal interview). WPAFB, 18 September 1980.

VITA

Gregory A. Mullins was born on 5 August 1952 in Dayton, Ohio. He graduated from high school in Fairborn, Ohio in 1970 and attended Wright State University from which he received the degree of Bachelor of Science in Systems Engineering in June 1974. Upon graduation, he was employed as Project Engineer for the Tri-Service Laser Seeker being developed for the USAF Laser Maverick Missile. He served in that position until entering the School of Engineering, Air Force Institute of Technology, in June 1979.

Permanent address: 5333 Grouse Court
Dayton, Ohio 45424

for the air-to-ground delivery of point-tracking weapons, the CO₂ system has the highest utility, followed by the Nd:YAG system. The millimeter wave system exhibits very poor utility because of its large beam divergence.

DATE
FILMED
-8-